ELSEVIER

Palaeogeography, Palaeoclimatology, Palaeoecology 202 (2003) 153–178

PALAEO

www.elsevier.com/locate/palaeo

Assimilation and transpiration capabilities of rhyniophytic plants from the Lower Devonian and their implications for paleoatmospheric CO_2 concentration

Anita Roth-Nebelsick *, Wilfried Konrad

Institut für Geowissenschaften der Universität Tübingen, Sigwartstr. 10, D-72076 Tübingen, Germany

Received 23 April 2002; received in revised form 13 August 2003; accepted 5 September 2003

Abstract

The characteristic basic construction of early land plants with an upright posture is represented by a simple leaf- and rootless axis system with a central conducting bundle ('rhyniophytic habit'). Variations of this simple architectural principle in different early land plant taxa probably reflect different ecophysiological requirements. In this contribution, the assimilation and transpiration of three different Rhynie Chert taxa (Pragian, Lower Devonian) which show this fundamental construction are analyzed in detail: *Aglaophyton major*, *Rhynia gwynne-vaughanii* and *Nothia aphylla*. The analysis was conducted by applying a simulation method based on diffusion through a porous material. The results demonstrate that the capability of gaseous exchange increases from *A. major* to *R. gwynne-vaughanii* to *N. aphylla*. *A. major* shows the most strict water-conserving strategy of the three taxa. The results are consistent with data from the fossil record concerning ecophysiological strategies and life styles. Furthermore, the results indicate clearly that the structural properties of early land plants reflect an optimization strategy with a fine-tuning of gaseous exchange. The rhyniophytic habit is strongly adapted to and dependent on high atmospheric CO_2 concentrations. The results provide evidence that the atmospheric CO_2 concentration of the Lower Devonian amounted to roughly 120 mmol/m^3.
© 2003 Elsevier B.V. All rights reserved.

Keywords: Lower Devonian; Plantae; Photosynthesis; Paleoecology; Paleoclimatology

1. Introduction

The earliest land plants which possessed an upright posture showed a rather uniform body structure. They consisted of a system of dichotomously branching leaf- and rootless axes with terminal sporangia and a central conducting bundle (see, for example, Stewart and Rothwell, 1993). This 'telomic' system represents very probable the constructional basis leading to modern cormophytes (extant plants composed of roots, stem and leaves) after several morphological transformations. It is widely accepted that all land plants including mosses, lycophytes and horsetails represent descendants of early land plants with such a rhyniophytic habit (Zimmermann, 1959; Kenrick and Crane, 1997; Bateman et al., 1998). The sys-

* Corresponding author. Tel.: +49-7071-2973561; Fax: +49-7071-295217.
E-mail address: anita.roth@uni-tuebingen.de (A. Roth-Nebelsick).

0031-0182/03/$ – see front matter © 2003 Elsevier B.V. All rights reserved.
doi:10.1016/S0031-0182(03)00634-5

tematic affinities of early land plants are complex and there is clear evidence that plants with a rhyniophytic habit belonged to different systematic groups. A rhyniophytic organization was expressed, for example, by the Rhyniopsida and several basal members of the Lycophytina (see thorough discussion in Kenrick and Crane, 1997). The term 'rhyniophytic' will thus be used here not in a systematic sense but in order to denote the telomic organization.

Despite fundamental differences between rhyniophytic plants and extant cormophytes, certain tissues of rhyniophytic plants are similar to tissues of modern land plants (Edwards, 1993; Remy and Hass, 1996; Edwards et al., 1998). Rhyniophytic plants show parenchyma with intercellular air spaces, stomata, cuticle and water transport tissue which is arranged within the central protostele. Rhyniophytic plants were thus equipped with all devices necessary for maintaining a homoiohydric state (Raven, 1984, 1993; Edwards et al., 1998). At first glance, the typical and uniform structure of 'characteristic' rhyniophytic plants appears to suggest correspondingly uniform ecophysiological properties. Recent findings of macrofossils of early land plants document, however, that early land plants were able to colonize various habitats with numerous survival strategies and functional adaptations (for example, Edwards, 1998; Edwards et al., 2001; Gerrienne et al., 2001). It was, for example, suggested by Gerrienne et al., 2001, that unusual spines on the axes of Lower Devonian plants existing in higher paleolatitudes were involved in freezing avoidance.

Well preserved plants of the Rhynie Chert also document numerous differences in tissue fine structure and morphology as well as in the habitats which were settled by different taxa (Edwards et al., 1998; Kerp et al., 2001). *Aglaophyton*, for example, produced more massive axes than *Rhynia*. The aerial axes of the systematically problematic *Nothia aphylla*, which was originally placed within the Rhyniopsida and is now classified as a plesiomorphic member of the Lycophytina, shows a rough surface strewn with protuberances (Kerp et al., 2001). The stomata are located on the summit of these protuberances. Furthermore, *Nothia* shows a much more intense underground rhizome system than *Aglaophyton* and *Rhynia*. An important question which will be addressed in this paper is whether or not these differences indicate significantly different ecophysiological requirements which reflect different ecological niches settled by Rhynie Chert taxa.

Any attempt to approach early land plant ecophysiology has to take paleoenvironmental conditions into account. One of the outstanding aspects of the early and lower middle Paleozoic climate is represented by the high atmospheric CO_2 concentrations, compared to the Recent conditions. During the Lower Devonian, for example, the atmosphere contained about 10 times more CO_2 than today, although the error range concerning this value is considerably high (Berner and Kothvala, 2001). Since the rhyniophytic habit represents the starting point of modern plants and because it evolved under – compared to Recent conditions – extremely high atmospheric CO_2 concentrations, an improvement of our knowledge about possible ecophysiological profiles of these archaic plants is valuable. One aspect of this consideration is the fact that stomatal densities of early land plants including rhyniophytic plants were utilized as proxy data of past atmospheric CO_2 concentrations (McElwain, 1998).

In this contribution, a detailed study of gaseous exchange of rhyniophytic plants is presented. Since experimental studies on fossil plants are impossible, theoretical methods are necessary. Calculations or simulations of assimilation and transpiration of early land plants were undertaken in some earlier studies. Raven (1984, 1993), for example, carried out calculations of gaseous exchange of early land plants. Beerling and Woodward (1997) applied an approach which couples photosynthesis and CO_2 influx. Description of molecular fluxes in analogy to electrical networks is a widely used concept. This method, however, produces correct results only if the pathways of the molecules can be described as straight lines (as is the case with flat leaves) and if no molecules are extracted from the diffusional gas flow. Rhyniophytic plants are however axisymmetric and CO_2 is removed from the gas flux along the cortex tissue due to the process of assimilation.

An alternate approach using a porous model approximation based on an approach of Parkhurst and Mott (1990) and Parkhurst (1994) was thus formulated and applied in the present study. It allows for detailed considerations of differences in tissue organization and systematic parameter variations. The following taxa are considered in this paper: *Aglaophyton major*, *Rhynia gwynne-vaughanii* and *Nothia aphylla*. The limits and ranges of their gaseous exchange are explored and compared. Implications for the atmospheric CO_2 concentrations of the Lower Devonian are also regarded.

2. The model system

2.1. The mathematical approach

A thorough presentation and discussion of the theoretical approach is provided in Konrad et al. (2000) and only a short explanation will thus be given here. The system of equations is based on Fick's first law of diffusion:

$$\vec{j} = -D \operatorname{grad} C \tag{1}$$

where $\vec{j}$ (in mol/m^2/s) denotes the diffusional flux, D (in m^2/s) the constant of diffusion, C (in mol/m^3) the concentration and grad the differential operator grad $f := (\partial f/\partial x, \partial f/\partial y, \partial f/\partial z)$.

If a gas diffuses through a tissue, then the diffusional pathways represent a complex network, because molecules can only diffuse through the void spaces between cells. This effect can be included into Eq. 1 by substituting D by the parameter S, the conductance:

$$S := D\,\frac{n}{\tau^2} \tag{2}$$

with porosity $n = V_p/V$ (V_p = pore volume of tissue, V = total volume of tissue). The tortuosity τ represents the 'averaged' increase of the molecular pathway due to the existence of hindrances (i.e. cells) which cannot be crossed by the molecules and have to be by-passed.

The desired mathematical solution of the present problem is given by insertion of Eq. 1 into the principle of mass conservation. A partial differential equation results which cannot be solved analytically in its most general form. Therefore, some approximations were introduced: (1) the system is supposed to be axially symmetric, (2) only the stationary state is considered, and (3) the tissue is treated as a porous medium. Approximation (1) is reasonable, because a telome of a rhyniophytic plant shows axial symmetry. Approximation (2) has the consequence that rapid temporal changes in gaseous exchange cannot be calculated exactly. Due to the typical dimensions of rhyniophytic plants, however, any 'diffusional state' remaining constant for at least $\approx 10^{-2}$ s can be treated as stationary with high accuracy. Approximation (3) averages the discontinuous system of single cells and voids of a certain tissue into a fictitious continuous tissue with uniform porosity and tortuosity.

After application of all approximations, the following ordinary differential equation results:

$$\frac{1}{r}\frac{\mathrm{d}}{\mathrm{d}r}\left(r\frac{\mathrm{d}C}{\mathrm{d}r}\right) = -\frac{Q}{S} \quad S = \text{const.} \quad C = C(r)$$

$$Q = Q(r, C(r)) \tag{3}$$

and

$$j(r) = -S\frac{\mathrm{d}C(r)}{\mathrm{d}r} \tag{4}$$

In order to solve Eq. 3 we have to specify the sink term $Q = Q(r,C(r))$, which represents in the case of CO_2 the photosynthesis model. A widely used photosynthesis model introduced by Farquhar et al. (1980) will be used for this purpose. It is shortly presented in the Appendix. A detailed discussion of the mathematical aspects of the model (including the solution procedure) is provided in Konrad et al. (2000).

A model of stomatal closure is not included in the system. A stomatal regulation mechanism which optimizes transpirational water loss and CO_2 influx appears to be realized in many angiosperms (Cowan and Farquhar, 1977). Several models of stomatal behavior exist (Ball et al., 1987; Jones, 1992; Aphalo and Jarvis, 1993; Beerling and Woodward, 1995). These models are, however, only applicable to angiosperms. In more ancient plant groups, such as ferns or coni-

fers, stomatal behavior is different from typical angiosperm characteristics (see Robinson, 1994 and citations therein). The fern *Pteridium aquilinum*, for example, shows a very slow stomatal movement with a strong endogeneous rhythm (Jarvis and Penny, unpublished results, discussed in Robinson, 1994). *P. aquilinum* and *Osmunda regalis* do not react instantaneously by rapid stomatal closure on variations in leaf-to-air vapor pressure deficit as is the case with many angiosperms (Franks and Farquhar, 1999). Edwards et al. (1996) suggested that rhyniophytic plants probably did not show control mechanisms of stomatal closure which are identical to control systems in extant angiosperms. No data are available about the mechanism of stomatal closure in rhyniophytic plants (Edwards et al., 1998). Regarding these considerations, the formulation of a reasonable model concerning stomatal closure in early land plants is currently not feasible. The model simulations include, however, a study on the effect of stomatal closure on gaseous exchange of the rhyniophytic axis.

Gaseous exchange was assumed to occur only by diffusion through the stomatal pores. Diffusion through the cuticle was not considered. The possibility cannot be excluded that the cuticle of rhyniophytic plants permitted a certain amount of gaseous exchange. Although *Aglaophyton*, for example, shows a distinct cuticle of several μm, this does not necessarily imply impermeability with respect to H_2O diffusion, because the permeance of a cuticle is more dependent on content and distribution of waxes and thus on its biochemical composition than on its thickness (Becker et al., 1986; Edwards et al., 1996). In extant plants, it was shown that low rates of gaseous exchange can occur via the cuticle (Kerstiens, 1996). It was, however, suggested that in many of these experiments a significant portion of gas flow occurred through incompletely closed stomata (Kerstiens, 1996). The actual permeance of extant cuticles thus appears to be very low in general. In rhyniophytic plants, the extremely low stomatal density together with the occurrence of a hypodermal channel (in the case of *Rhynia* and *Aglaophyton*) suggest a constructional principle of severely controlled gaseous exchange and thus low cuticular transpiration, which was therefore neglected in the model.

The entire system of Eqs. 3–9 is applied to concentrically arranged layers representing the cross-sectional model of a rhyniophytic axis and includes the boundary layer, stomatal layer, hypodermal layer (if present) and outer cortex layer (see Fig. 1) (for Eqs. 5–9 see the Appendix). The final layer specific versions of Eqs. 3 and 4 are solved for each layer in such a way that the overall solution becomes a continuously differentiable function of r. The calculations were performed with the commercial computer code MAPLE. A detailed representation and discussion of the solution procedure is provided by Konrad et al. (2000).

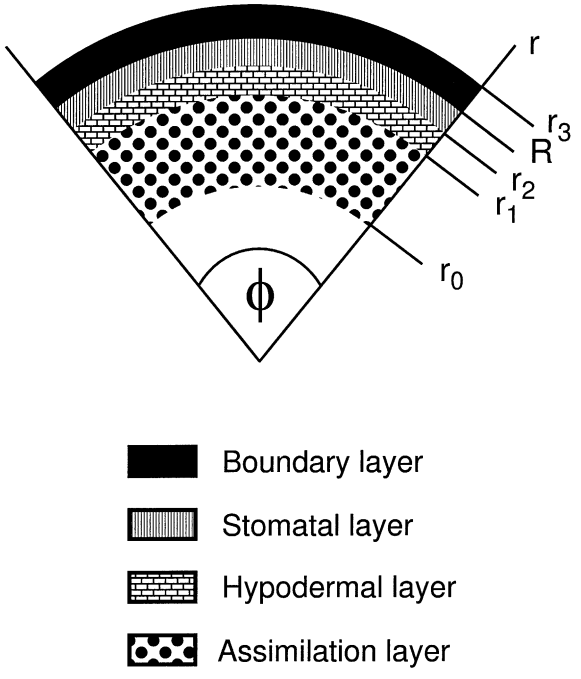

Fig. 1. Schematic representation of the tissue layer structure of the plant models. Only the tissue layers which are considered by the mathematical model are shown. Note that the radial dimensions of the layers in this illustration do not indicate real layer thickness. The z-axis (longitudinal axis) is orientated perpendicularly to the illustration. Black: boundary layer (R–r_3, R: plant radius); hatched: stomatal layer (r_2–R); ruled: hypodermal layer (r_1–r_2); dotted: assimilation layer (r_0–r_1). After Konrad et al., 2000.

2.2. Determination of parameters and sensitivity analyses

The simulations require several parameters of different classes: environmental, anatomical and biochemical. All parameters are listed in Tables 1–3 together with their sources. The values summarized in Tables 1–3 are termed 'initial data set' throughout the rest of the paper. The values of several parameters have to be derived from other parameters. These parameters are specially marked in the tables and the calculation methods are provided in the Appendix. For several parameters, the chosen values will be shortly discussed in the following section. All other parameter values will be discussed in Section 4.1.

The atmospheric CO_2 content is derived from model simulations which indicate R_{CO_2} values (R_{CO_2} = fossil CO_2 concentration/Recent CO_2 concentration) of the Lower Devonian between 10 and 15 (Berner and Kothvala, 2001). For the Pragian (age of Rhynie Chert) a value of $R_{CO_2} = 12$ is suggested by Berner and Kothvala (2001). For the initial data set, a CO_2 concentration 12 times higher than the Recent value was thus chosen. The best fit curve of past CO_2 concentrations is, however, enveloped by an error range of considerable size (Berner and Kothvala, 2001). Possible implications of the present results for estimations of Lower Devonian CO_2 concentrations are discussed in Section 4.4.

The irradiance value is based on the Recent solar constant and the various processes of scattering and reflection of electromagnetic radiation back into space (see, for example, Gates, 1980 or Nobel, 1999). The amount of visible light which is then absorbed by the plant axis is calculated according to the elevation of the sun and by taking the cylindric shape into account (see method in the Appendix) (Niklas and Kerchner, 1984).

Most of the anatomical parameters are obtained from the literature dealing with excellently preserved specimen from the Rhynie Chert, Scotland or from our own measurements. These permineralized specimen allow for reliable reconstructions of axis diameter, geometric properties or thickness of tissue layers, such as width of stomatal pore or thickness of epidermis, as well as the determination of tissue porosity. Since chloroplasts are, however, not preserved by fossilization processes, the surface factor of the chloroplasts has to be estimated on the basis of data from extant plants (see description in the Appendix).

All biochemical parameters have to be taken from corresponding literature data obtained for extant plants. V_{max} and J_{max}, for example, were taken from the range of values found for extant conifers and then fine-tuned in such a way that the ratio between internal and external CO_2 concentration amounts to $C_i/C_a = 0.7$. It is generally assumed that this ratio represents – at least on an averaging long-term scale – a common value realized in land plants (Kürschner, 1996; Beerling and Woodward, 1997). The values of V_{max} and J_{max} are in this case at the lower range of values found in extant conifers (see Appendix). The reliability of the biochemical parameters is discussed in Section 4.

The present contribution contains several sensi-

Table 1
The environmental parameters of the simulation model

Parameter	Value	Source
Wind velocity u_{atm} (m/s)	0.8	arbitrary
Boundary layer thickness d_{bl} (10^{-3} m)		derived
Atmospheric CO_2 content C_a (mmol/m^3)	168	Berner and Kothvala, 2001
Atmospheric H_2O content $C_{atm}^{H_2O}$ (mmol/m^3)[a]	843	arbitrary
Air temperature T (°C)	30	Beerling et al., 2001
Irradiance $I_{\Theta=45°}$ (μmol/m^2/s)	620	arbitrary

In the case of the derived parameters, the method of calculation is provided in the Appendix.
[a] Parameter is varied, see text.

Table 2
The anatomical parameters of the simulation model

Parameter	*Aglaophyton*	*Rhynia*	*Nothia*
Radius of plant R (10^{-3} m)[a]	2.25	1.0	1.050[b]
Depth of stomatal pore d_{st} (10^{-3} m)[c,d,e]	0.03	0.015	0.03
Long axis of stoma h_{st} (10^{-3} m)[c,d]	0.039	0.029	0.021
Short axis of stoma w_{st} (10^{-3} m)[c,d]	0.0105	0.01	0.0025
Area of stomatal pore a_{st} (10^{-10} m^2)[c,d,e]	3.216	2.278	0.412
Stomatal density v_{st} (10^6/m^2)[d,f]	1.0	1.75	3.35
Porosity of stomatal layer n_{st} (10^{-3})[f,g]	0.32	0.399	0.357
Tortuosity of stomatal layer τ_{st} (10^{-3})[f,g]	1.34	1.57	1.12
'Conductivity'[h] of stomatal layer n_{st}/τ_{st}^2 (10^{-3})[g,h]	0.18	0.16	0.28
Thickness of hypodermal layer d_{hc} (10^{-3} m)[c,d,f]	0.075	0.105	–
Long axis of hypodermal channel h_{hc} (10^{-3} m)[c,d,e]	0.04	0.03	–
Short axis of hypodermal channel w_{hc} (10^{-3} m)[c,d,e]	0.03	0.02	–
Area of hypodermal channel a_{hc} (10^{-10} m^2)[c,d,e]	9.42	4.71	–
Porosity of hypodermal layer n_{hc} (10^{-3})[f,g]	0.96	0.87	–
Tortuosity of hypodermal layer τ_{hc} (10^{-3})[f,g]	1.0	1.0	–
'Conductivity'[h] of hypodermal layer n_{hc}/τ_{hc}^2 (10^{-3})[f,g]	0.96	0.87	–
Thickness of assimilation layer d_{as} (10^{-3} m)[c,d]	0.25	0.1	0.42[i]
Cortex cell radius σ (10^{-6} m)[c,d]	55	50	45
Specific surface of cortex cell (a_{as}/v_{as}) (1/m)[g]	36 364	40 000	44 444
Surface factor of chloroplasts (a_{chl}/a_{as}) (–)[g]	2.345	2.345	2.345
Porosity of assimilation layer n_{as} (10^{-3})[j]	0.35	0.35	0.35
Tortuosity of assimilation layer τ_{as} (10^{-3})[g]	1.571	1.571	1.571
'Conductivity'[h] of assimilation layer n_{as}/τ_{as}^2 (10^{-3})[f,g]	0.142	0.142	0.142

In the case of the derived parameters, the method of calculation is provided in the Appendix.

[a] Various sources.

[b] In the case of *Nothia* this indicates the 'outer' radius of the plant (i.e. including *Nothia*'s emergences). The 'inner' radius (measured at the bases of the emergences) amounts to 0.72 10^{-3} m.

[c] Edwards et al., 1998.

[d] Kerp et al., 2001.

[e] Kerp and Hass, personal communication.

[f] Parameter is varied, see text.

[g] Parameter is derived.

[h] The conductance $S = Dn/\tau^2$ splits up into a factor D containing properties of the diffusing substance and a factor n/τ^2 describing the morphology of the medium. The term 'conductivity' stands for the second factor.

[i] In the case of *Nothia* the emergences are supposed to contain assimilating tissue.

[j] Parameter was obtained by own measurements.

tivity analyses. During a sensitivity analysis, one or two parameters are varied systematically, while the others are kept constant. Sensitivity analyses are valuable in order to, (1) analyze system behavior, and (2) check the reliability and limitations of the model approach. If a sensitivity analysis is carried out, then the varied parameters are explicitly described in the corresponding sections, while the other parameters show the values provided in the initial data set listed in Tables 1–3.

3. Results

3.1. Local fluxes of H_2O and CO_2 with initial data set

The flux of H_2O is caused only by the water potential gradient between plant tissue and atmosphere whereas for CO_2 the flux is generated by the assimilation process. Fig. 2 shows the local fluxes of CO_2 and H_2O for *Aglaophyton*, *Rhynia* and *Nothia* for the initial data set, plotted against

Table 3
The biochemical parameters of the simulation model

Parameter	*Picea*	*Aglaophyton*	*Rhynia*	*Nothia*
Effective conductance through a cortex cell g_{liq} (10^{-3} mmol/m^2/s/Pa)	0.5	0.5	0.5	0.5
Light-saturated rate of electron transport J_{max} (10^{-3} mmol/m^2/s)[a]	2.048	1.047	2.884	0.792
Michaelis–Menten constant for carboxylation K_c (Pa)	189	189	189	189
Michaelis–Menten constant for oxygenation K_o (Pa)	42 382	42 382	42 382	42 382
Local maximum carboxylation rate V_{max} (10^{-3} mmol/m^2/s)[a]	0.842	0.430	1.185	0.325
Partial pressure of oxygen at chloroplasts p_o (Pa)	20 260	20 260	20 260	20 260
Efficiency of light conversion α (–)	0.2	0.2	0.2	0.2
Specificity factor for Rubisco θ (–)	1 906	1 906	1 906	1 906

The values of the local maximum carboxylation rate V_{max} and of the light-saturated rate of electron transport J_{max} labeled *Aglaophyton*, *Rhynia* and *Nothia*, respectively, are calculated in such a way that the condition $C_i/C_a = 0.7$ is fulfilled.
The data are compiled from the following sources: Harley and Sharkey, 1991; Harley et al., 1992; Kirschbaum and Farquhar, 1984; Parkhurst and Mott, 1990; Wullschleger, 1993.
[a] Parameter is varied, see text.

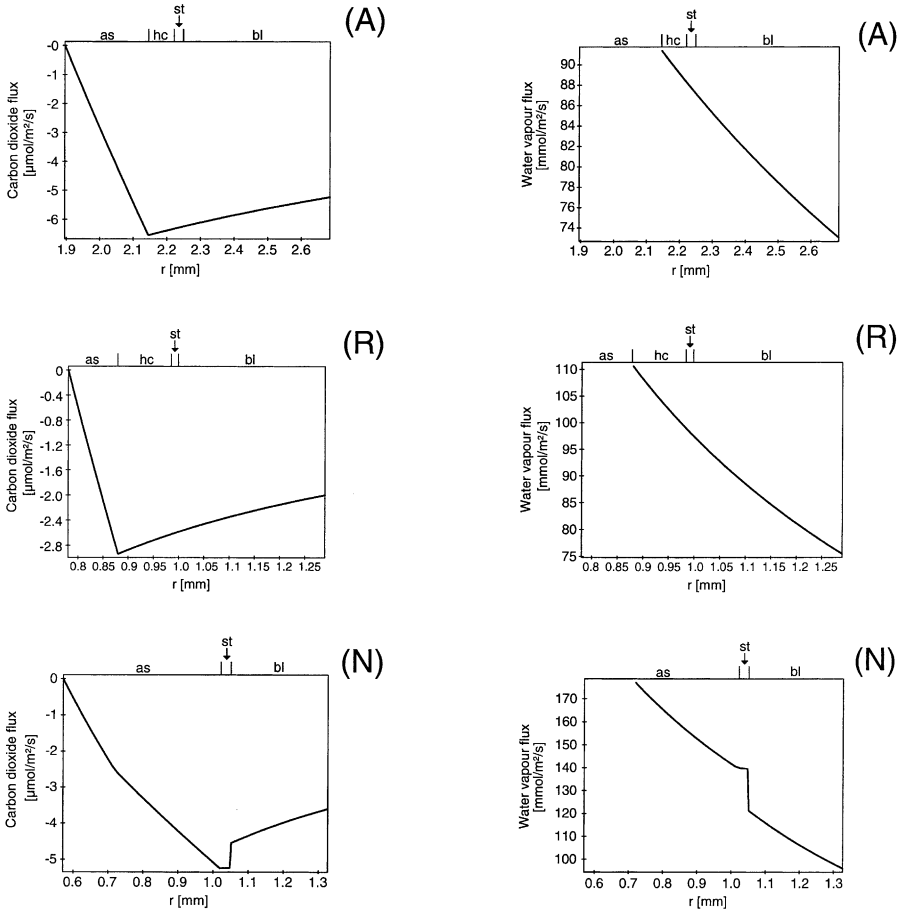

Fig. 2. Local fluxes of H_2O and CO_2 plotted against radial coordinate for *Aglaophyton major* (A), *Rhynia gwynne-vaughanii* (R) and *Nothia aphylla* (N). as, hc, st and bl are abbreviations for assimilation layer, hypodermal channel, stomatal layer and boundary layer, respectively.

the distance r from the symmetry axis (listed in Tables 1–3). For *Aglaophyton* and *Rhynia*, the fluxes of H_2O and CO_2 (outside the assimilation layer) are smooth functions of r. This is due to, (1) the axial symmetry of the plant, and (2) the principle of conservation of mass which forces the fluxes to increase or decrease inversely proportional to r if sources or sinks are absent. In the case of *Nothia*, the fluxes behave somewhat less smoothly, because *Nothia*'s emergences destroy the complete axial symmetry of the plant axes. Inside the assimilation layer, the CO_2 flux changes for all three species from an increase to a strong decrease due to the consumption of CO_2 during the assimilation process. Fig. 3 shows the local concentrations of H_2O and CO_2. Strong gradients are visible along: (1) the stomatal pore and (2) the hypodermal channel (in the cases of *Aglaophyton* and *Rhynia*). In the case of CO_2, a gradient along the assimilation layer has established. It is, however, weak if compared to the stomatal and hypodermal gradient. The initial values of V_{max} and J_{max} lead to values of intercellular CO_2 concentration of about $C_i/C_a = 0.7$ (see Section 2.2). Assimilation is saturated under these conditions.

3.2. Transpiration and assimilation rates with initial data set

The transpiration rate (i.e. the efflux of H_2O

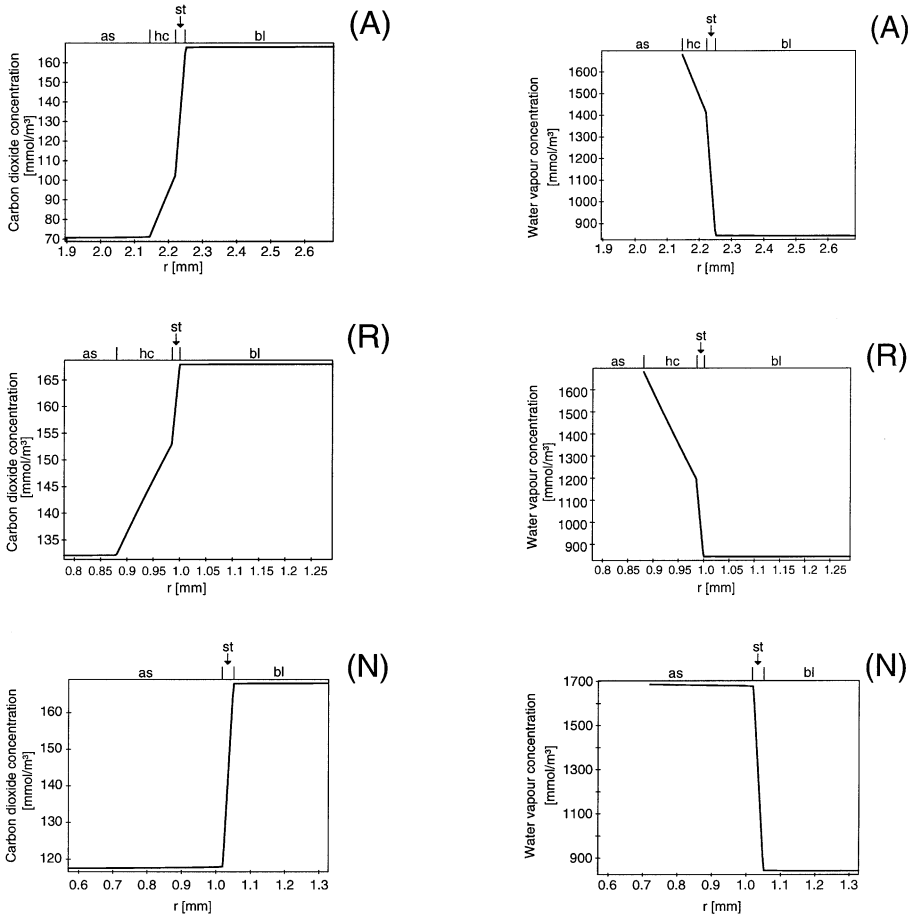

Fig. 3. Local concentrations of H_2O and CO_2 plotted against radial coordinate for *Aglaophyton major* (A), *Rhynia gwynne-vaughanii* (R) and *Nothia aphylla* (N). as, hc, st and bl are abbreviations for assimilation layer, hypodermal channel, stomatal layer and boundary layer, respectively.

out of the axis surface per unit surface area) for *Aglaophyton*, *Rhynia* and *Nothia* is plotted as a histogram in Fig. 4. *Aglaophyton* and *Rhynia* show similar transpiration rates. *Nothia* shows the highest transpiration rate. The transpiration is low for all three taxa compared to common values of extant plants. *Aglaophyton*, for example, transpires 0.087 mmol/m^2/s whereas for leaves of mesophytic trees values of 3 mmol/m^2/s are common (see, for example, Larcher, 1997). It is, however, more reasonable in the case of rhyniophytic plants to relate their water loss to their volume (see underlying ideas in Section 4.2). This is accomplished by calculating $\mathcal{T} = j^{H_2O}(R) \times 2\pi RL/(\pi R^2 L) = 2/R \times j^{H_2O}(R)$ where L denotes the axis length. The results are included in Fig. 4. In this case, *Aglaophyton* shows the lowest transpiration rate, *Nothia* develops again the highest rate, while *Rhynia* lies in between these two values.

Fig. 5 shows the values of CO_2 influx per unit surface area into the plant axes for *Aglaophyton*, *Rhynia* and *Nothia*. The CO_2 influx values represent the assimilation rates. Assimilation is highest for *Nothia* and lowest for *Aglaophyton* with *Aglaophyton* and *Rhynia* showing similar values. Note that the CO_2 influx is not related to projected surface area as is usual for assimilation rates of extant plants. Converting assimilation rates per projected surface area to allow for the direct comparison with literature data of extant plants requires the multiplication of the presented values with the factor 4.44 (because of $2\pi RL/(2RL \cos \Theta) = \pi/\cos \Theta = 4.44$, if the sun is elevated $\Theta = 45°$ above the horizon and with an axis of length L). If the assimilation is, however, related to volume by the same procedure as was applied in the case of the water efflux (see above and underlying ideas in Section 4.2), then *Aglaophyton* shows a distinctly lower value than *Rhynia* while *Nothia* develops again the highest value (see Fig. 5). The formal definition of the assimilation rate per volume is given by $\mathcal{A} = j^{CO_2}(R) \times 2\pi RL/(\pi R^2 L) = 2/R \times j^{CO_2}(R)$.

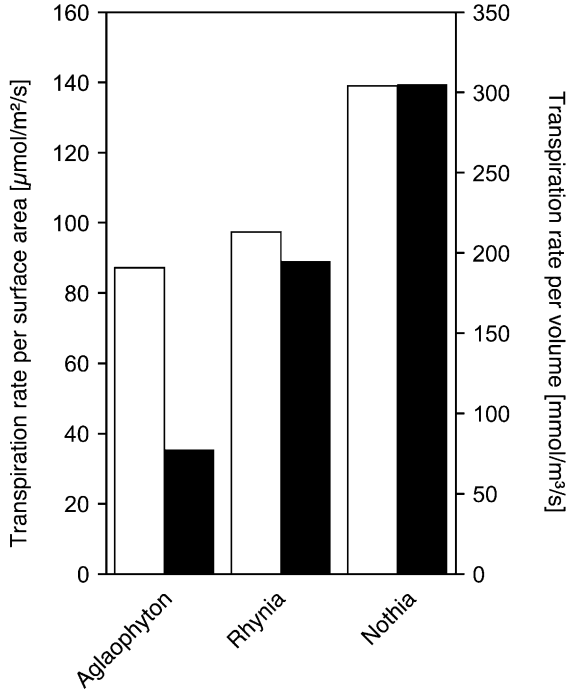

Fig. 4. Transpiration rates of *Aglaophyton major*, *Rhynia gwynne-vaughanii* and *Nothia aphylla*. White columns: transpiration rate per surface area (µmol/m^2/s). Black columns: transpiration rate per volume (mmol/m^3/s).

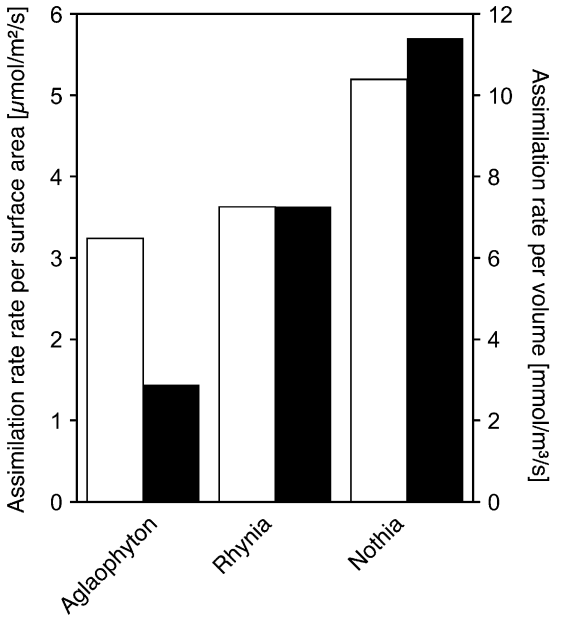

Fig. 5. Assimilation rates of *Aglaophyton major*, *Rhynia gwynne-vaughanii* and *Nothia aphylla*, obtained with V_{max} and J_{max} from the initial data set. White columns: assimilation rate per surface area (µmol/m^2/s). Black columns: assimilation rate per volume (mmol/m^3/s).

The parameter of WUE ('water use efficiency') gives the ratio between the numbers of assimilated CO_2 molecules and transpired H_2O molecules. It is usually expressed as µmol CO_2 fixed per mmol H_2O lost. The value of WUE represents the instantaneous water loss during photosynthesis and is therefore strongly dependent on various parameters, such as the degree of stomatal closure, temperature or relative humidity. In a real plant, the WUE thus represents a strongly fluctuating parameter whose instantaneous value changes with various factors. In order to obtain a long-term value of net carbon gain, long-term parameters, such as the seasonal amount of water transpired per dry matter produced, are often used especially in agricultural studies (Kramer, 1983). It is, however, possible to obtain 'characteristic' WUE values of extant and unstressed C_3 plants with their stomata fully opened (Nobel, 1999). With the initial data set, the calculated assimilation and transpiration rates of *Aglaophyton*, *Rhynia* and *Nothia* yield values around WUE ≈ 37, which is about 18 times higher than the 'typical' extant value. Similar WUE values for all three plants under the conditions of the initial data set are to be expected as the WUE depends – at least approximately – not on the morphology of a plant but rather on the ratio of the (free air) diffusional constants with respect to CO_2 and H_2O times the ratio of the concentration gradients of CO_2 and H_2O, i.e. $WUE = D^{CO_2}/D^{H_2O} \times \Delta C^{H_2O}/\Delta C^{H_2O}$ (Farquhar et al., 1989).

3.3. Sensitivity analyses

3.3.1. Variation of V_{max} and J_{max}

With the present V_{max} and J_{max} values, small variations of these two parameters lead to strong changes of the assimilation rate. In order to perform a sensitivity analysis with respect to V_{max} and J_{max}, different values of these two parameters were inserted. By doing this, the concept of $C_i/C_a = 0.7$ is dismissed. For this sensitivity analysis, V_{max} and J_{max} values of a certain extant conifer (*Picea abies*, Wullschleger, 1993) are applied ($V_{max} = 0.842$ µmol/m²/s and $J_{max} = 2.05$ µmol/m²/s) instead of the values of the initial data set (see Table 3, note that the original literature data have been transformed according to rhyniophytic anatomical structure, see Appendix). These values were chosen, because V_{max} and J_{max} of conifers are rather low and it is reasonable to assume that V_{max} and J_{max} of rhyniophytic plants were located at the lower range of the extant spectrum of assimilation parameters (see Section 4.1.2).

With these values, *Aglaophyton* exhibits distinctly higher assimilation rates per surface area than *Rhynia* (see Fig. 6). If related to axis volume, however, *Aglaophyton* and *Rhynia* show almost identical values (see Fig. 6). The assimilation rate of *Nothia* approximately doubles on replacing the V_{max} and J_{max} values of the initial data set by the *Picea abies* values and attains again the highest value of all three taxa, both with respect to surface area and to volume (see Fig. 6). The WUE values change in accordance with the assimilation rates, because the transpiration rate is not influenced by the values of V_{max} and J_{max} (see Fig. 7). The ratios of internal CO_2 concentration to external CO_2 concentration now amount to

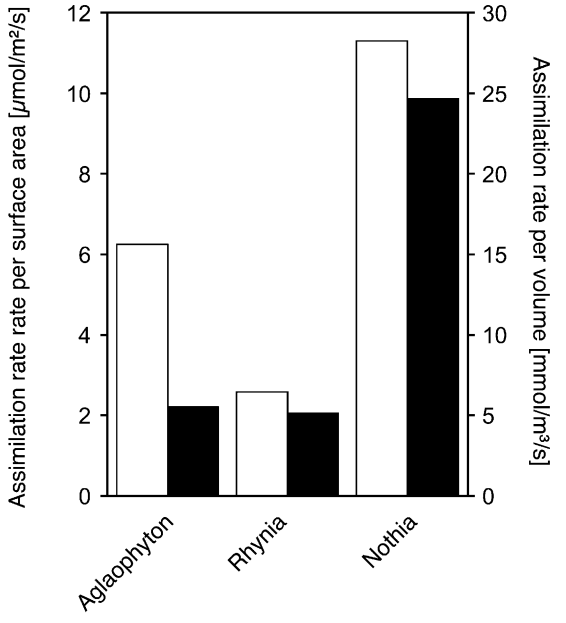

Fig. 6. Assimilation rates of *Aglaophyton major*, *Rhynia gwynne-vaughanii* and *Nothia aphylla*, obtained with V_{max} and J_{max} from *Picea abies*. White columns: assimilation rate per surface area (µmol/m²/s). Black columns: assimilation rate per volume (mmol/m³/s).

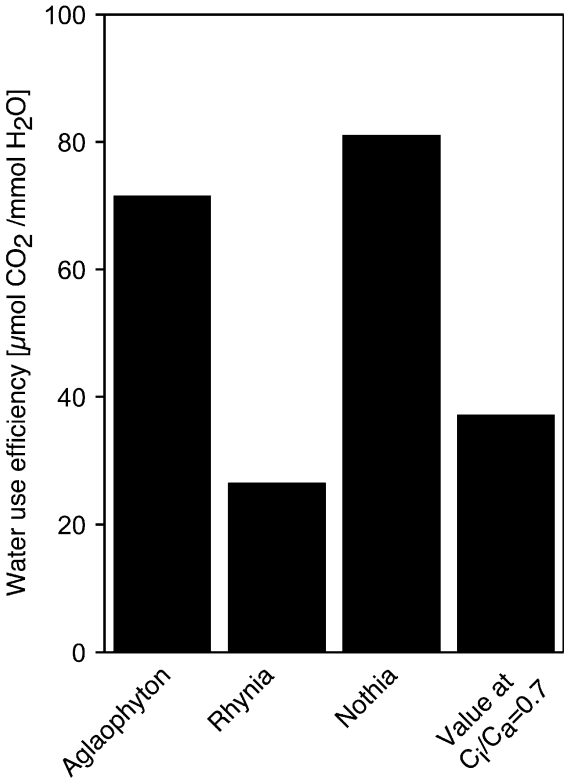

Fig. 7. Values of WUE of *Aglaophyton major*, *Rhynia gwynne-vaughanii* and *Nothia aphylla*. Values of V_{max} and J_{max} from *Picea abies* lead to different values of WUE for each species (left three columns). Values of V_{max} and J_{max} from the initial data set (derived via the condition $C_i/C_a = 0.7$) result in a common WUE value for all three species (right column).

$C_i/C_a = 0.42$ for *Aglaophyton*, $C_i/C_a = 0.79$ for *Rhynia* and $C_i/C_a = 0.35$ for *Nothia*. The reason for the strong effect of this moderate variation of V_{max} and J_{max} is illustrated by Fig. 8 which shows the CO_2 influx as depending on V_{max} and J_{max}. The initial values of V_{max} and J_{max} are located at the critical 'flank' and small variations of these two values thus result in strong changes of the CO_2 influx.

3.3.2. Variation of stomatal density, thickness of hypodermal channel and stomatal opening

The assimilation rate plotted against length of the hypodermal channel d_{hc} and stomatal density ν_{st} for *Aglaophyton* is shown in Fig. 9a. The ranges are $d_{hc} = 0...1.05$ mm and $\nu_{st} = 0...20/m^2$. All other values correspond to the initial data set. The graph illustrates the threshold behavior of the assimilation rate with respect to the parameter ν_{st}. Below the threshold value of ν_{st}, the assimilation rate decreases strongly with decreasing ν_{st} and changes with d_{hc} in a non-linear manner. Above the threshold value, an increase in ν_{st} has

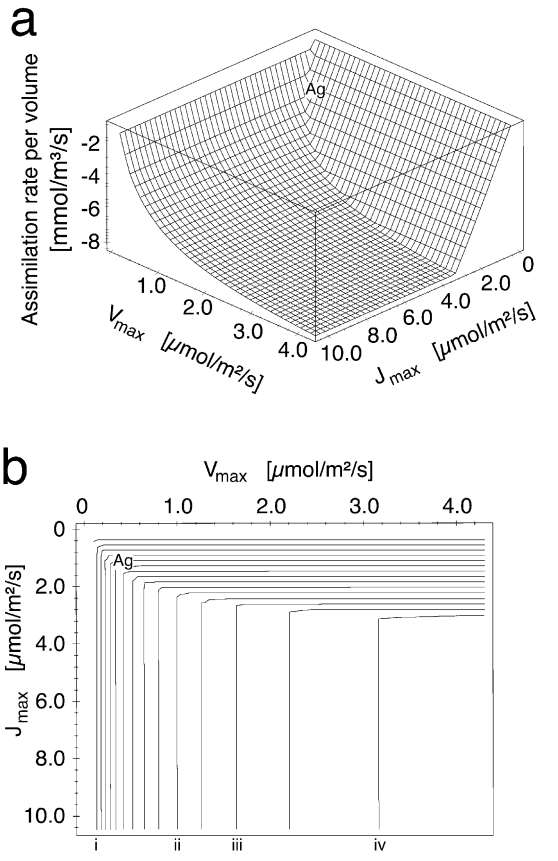

Fig. 8. a: Sensitivity analysis: dependence of assimilation rate per volume on V_{max} and J_{max} for *Aglaophyton major* plotted in a three-dimensional representation. The position of the result obtained with the initial data set is indicated in the graph by the mark 'Ag'. b: Sensitivity analysis: dependence of assimilation rate per volume on V_{max} and J_{max} for *A. major* plotted in a two-dimensional representation (contour plot). The graph can be described as top view of Fig. 8a. The lines are lines of constant assimilation rate per volume. The lines marked i to iv represent the following assimilation rates per volume: -1.5 mmol/m^3/s, -6 mmol/m^3/s, -7 mmol/m^3/s and -8 mmol/m^3/s, respectively. Values of adjacent lines differ by 0.5 mmol/m^3/s. The position of the result obtained with the initial data set is indicated in the graph by the mark 'Ag'.

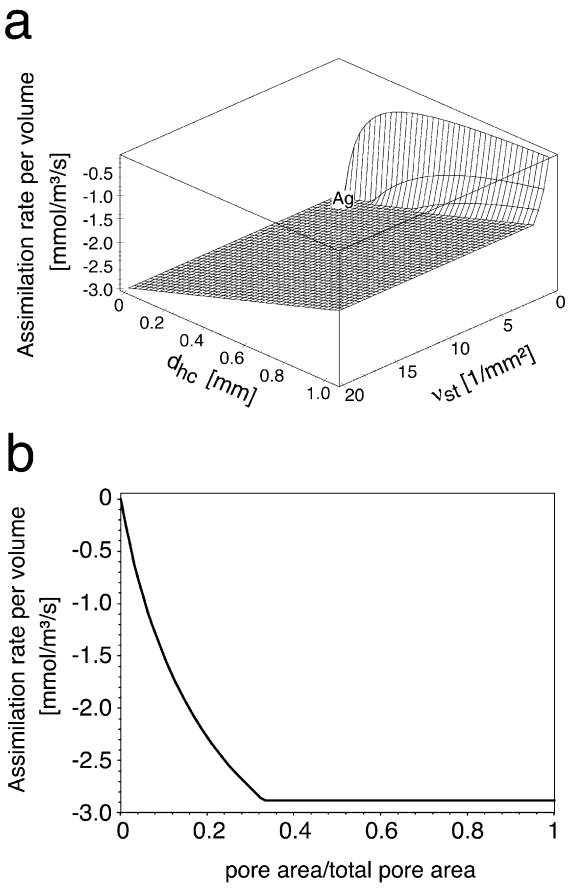

Fig. 9. a: Sensitivity analysis: assimilation rate per volume plotted against length of hypodermal channel d_{hc} and stomatal density ν_{st} for *Aglaophyton major*. The position of the result obtained with the initial data set is indicated in the graph by the mark 'Ag'. b: Sensitivity analysis: assimilation rate per volume plotted against degree of stomatal closure, expressed as ratio between pore area and total pore area. This ratio can take values between 0 (= fully closed stomata) and 1 (= fully opened stomata).

no significant effect on assimilation, whereas the assimilation rate increases approximately linearly with decreasing d_{hc}. The same behavior can be observed for *Rhynia* and *Nothia* (data not shown). For all three plants, the (calculated) threshold values of ν_{st} are close to the (measured) values which were used in the initial data set.

Fig. 9b shows the change of assimilation rate during stomatal closure which is provided in the figure as ratio between the pore area and the area of the completely opened pore (the value of 1 represents thus fully opened stomata). Fig. 9b demonstrates that the assimilation rate increases strongly when the pore begins to open and reaches a plateau at a degree of stomatal opening of about 0.3 (= 30%). Further increase in stomatal opening does not result in increasing assimilation rates.

Fig. 10a depicts how the transpiration rate of *Aglaophyton* depends on d_{hc} and ν_{st}. d_{hc} and ν_{st} are varied across the same ranges as in the sensitivity analysis of the assimilation rate. For $d_{hc} \lessapprox 0.2$ mm and for $\nu_{st} \lessapprox 1.5/\text{mm}^2$, the transpira-

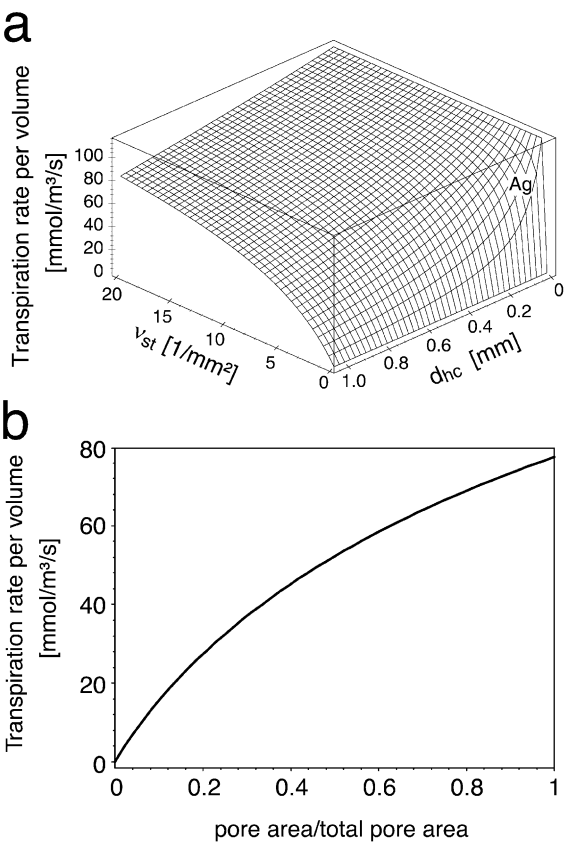

Fig. 10. a: Sensitivity analysis: transpiration rate per volume plotted against length of hypodermal channel d_{hc} and stomatal density ν_{st} for *Aglaophyton major*. The position of the result obtained with the initial data set is indicated in the graph by the mark 'Ag'. b: Sensitivity analysis: transpiration rate per volume plotted against degree of stomatal closure, expressed as ratio between pore area and total pore area. This ratio can take values between 0 (= fully closed stomata) and 1 (= fully opened stomata).

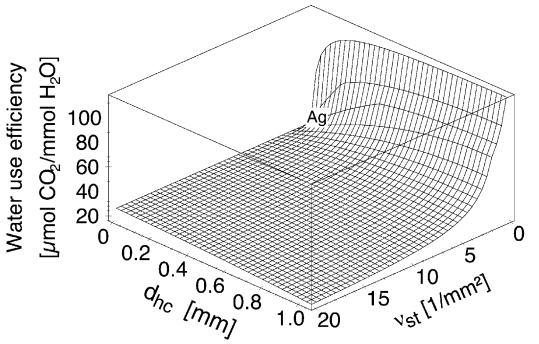

Fig. 11. Sensitivity analysis: WUE plotted against length of hypodermal channel d_{hc} and stomatal density ν_{st} for *Aglaophyton major*. The position of the result obtained with the initial data set is indicated in the graph by the mark 'Ag'.

tion rate varies strongly and in a non-linear manner on both ν_{st} and d_{hc}. With higher values of the stomatal density, the transpiration reacts more moderately on changes in ν_{st} and d_{hc}. Inspection of Fig. 10a reveals that the 'actual' transpiration rate of *Aglaophyton* is located at the upper end of the steep flank. The same behavior can be observed for *Rhynia* and *Nothia* (data not shown). In Fig. 10b the change of transpiration rate during stomatal closure is represented. It can be seen that – contrary to the change in assimilation rate, shown in Fig. 9b – the transpiration rate increases smoothly with increasing stomatal opening. At a degree of stomatal opening of roughly 0.3 – which suffices for achieving maximum assimilation rate – the transpiration rate amounts to about half the value of transpiration with fully open pores.

The WUE (which can, by definition, be viewed as combining effects of assimilation rate and transpiration rate) is shown as a function of d_{hc} and ν_{st} in Fig. 11. A steep flank develops for $\nu_{st} \lessapprox 1.5/\text{mm}^2$ and $d_{hc} \lessapprox 0.2$ mm. The WUE value obtained with the initial data set is seated at the bottom of this flank.

3.3.3. *Variation of atmospheric CO_2 concentration*

The assimilation rates are plotted against the atmospheric CO_2 concentration C_a for the range $C_a = 10...250$ mmol/m^3 in Fig. 12a,b. V_{max} and J_{max} values correspond to the initial data set (Fig. 12a) or are taken from extant *Picea abies* (Fig. 12b) (see Section 3.3.1). In the horizontal segments (i.e. parallel to the abscissae) of the curves photosynthesis is saturated, in the inclined parts it is undersaturated. Under the conditions of the initial data set, saturation of photosynthesis starts at $C_a \approx 120$ mmol/m^3 (Fig. 12a). For V_{max} and J_{max} of *Picea*, starting points of saturated photosynthesis are located at $C_a \approx 106$ mmol/m^3 (*Rhynia*), $C_a \approx 166$ mmol/m^3 (*Aglaophyton*), and $C_a \approx 193$ mmol/m^3 (*Nothia*) (Fig. 12b).

In another sensitivity analysis, C_a and ν_{st} are varied simultaneously. With the other values corresponding to the initial data set, Fig. 13a,b shows the result for *Aglaophyton*. A large, plain 'floor' represents combinations of C_a and ν_{st} which lead to saturation of photosynthesis, while

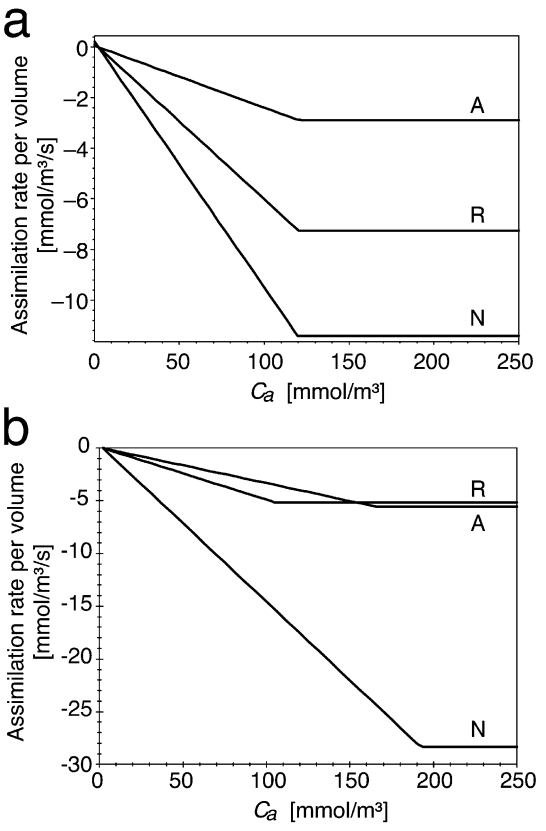

Fig. 12. Sensitivity analysis: assimilation rate per volume plotted against atmospheric CO_2 concentration C_a for *Aglaophyton major* (A), *Rhynia gwynne-vaughanii* (R) and *Nothia aphylla* (N). a: J_{max} and V_{max} of the initial data set (leading to $C_i/C_a = 0.7$). b: J_{max} and V_{max} of an extant plant (*Picea abies*).

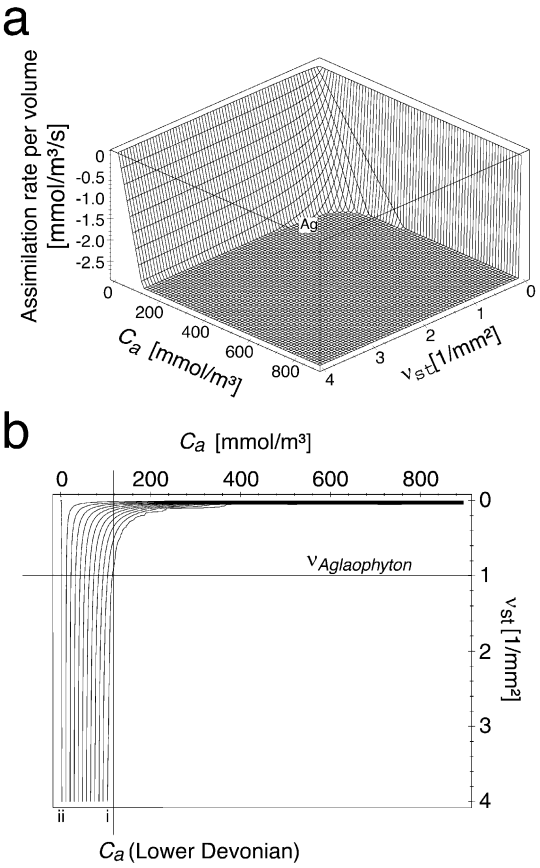

Fig. 13. a: Sensitivity analysis: assimilation rate per volume plotted against atmospheric CO_2 concentration C_a and stomatal density ν_{st} for *Aglaophyton major*. The position of the result obtained with the initial data set is indicated in the graph by the mark 'Ag'. b: Sensitivity analysis: assimilation rate per volume plotted against atmospheric CO_2 concentration C_a and stomatal density ν_{st} for *A. major* in a two-dimensional representation (contour plot). The graph can be described as top view of Fig. 13a. The lines are lines of constant assimilation rate per volume. The lines marked i and ii represent values of assimilation rate per volume of -2.75 mmol/m^3/s and 0 mmol/m^3/s, respectively. Values of adjacent lines differ by 0.25 mmol/m^3/s.

the two 'walls' result from strong variations of the assimilation rate for (C_a,ν_{st})-pairs which are too low to allow for saturation of photosynthesis. For $\nu_{st} \gtrapprox 1.4/\text{mm}^2$, saturation is nearly independent of ν_{st} and is given as long as $C_a \gtrapprox 120$ mmol/m^3 is fulfilled. $\nu_{st} \lessapprox 1.4/\text{mm}^2$, however, requires increasingly high values of C_a in order to keep photosynthesis saturated. For $C_a \gtrapprox 400$ mmol/m^2, the value of C_a has little influence on saturation, provided $\nu_{st} \gtrapprox 0.1/\text{mm}^2$ is satisfied. Variation of the photosynthesis parameters V_{max} and J_{max} changes the positions, where the 'undersaturated' walls raise from the 'saturated' floor, but not the qualitative features of the graph. If, for example, V_{max} and J_{max} of *Picea abies* are used, then $\nu_{st} \gtrapprox 1.5/\text{mm}^2$ requires $C_a \approx 160$ mmol/m^3 to saturate photosynthesis, and C_a loses its influence on saturation only for values of $C_a \gtrapprox 650$ mmol/m^2 (again under the premises $\nu_{st} \gtrapprox 0.1/\text{mm}^2$). *Rhynia* and *Nothia* show similar behavior.

3.3.4. *Variation of other photosynthesis parameters and chloroplast density*

There are some other parameters, which influence assimilation: the effective conductance through the interior structures of the cortex cells g_{liq}, the specificity factor for Rubisco θ, the irradiance I, the efficiency of light conversion α and the chloroplast surface factor a_{chl}/a_{as}.

In order to find out whether any of these parameters are critical (in the sense, that small deviations from their exact values result in high changes of the results) we performed sensitivity analyses by plotting the assimilation rate as a function of each of these variables while keeping the other variables constant. These graphs (not shown) have several features in common: (1) when the independent variable approaches zero, the assimilation rate disappears as well, (2) the assimilation rate increases continuously with increasing independent variable, and (3) all curves behave asymptotically, i.e. the assimilation rate is saturated for sufficiently high values of the independent variable. According to the positions, which are occupied by the parameter values of the initial data set, we draw the following conclusions: (1) g_{liq} and θ are uncritical, because their initial data set values are positioned on the asymptotic segment of the curves, (2) I and α are 'semi-critical' in the following sense: their initial data set values lie at the 'beginning' of the asymptotic segment, i.e. if their 'true' values would be higher than the values assigned to them in the initial data set, then this error would not influence the assimilation rate, but if the 'true' values would be lower, the initial data set would produce mis-

leadingly high results, (3) the chloroplast surface factor a_{chl}/a_{as} is critical: its initial data set value lies on the segment of the curve which exhibits the steepest gradient.

4. Discussion

4.1. Reliability of input parameters

4.1.1. Humidity, wind speed and temperature

Humidity and wind speed were arbitrarily chosen, because it is very probable that these parameters showed a similar wide range of values during the Lower Devonian as they do today. Humidity (i.e. atmospheric H_2O concentration) influences the results via the transpiration rate, because the evaporative water loss is proportional to the gradient of the water vapor concentration between the intercellular spaces of the plant and the atmosphere (see, for example, Jones, 1992 or Nobel, 1999). More precisely, transpiration rate is a linear function of the atmospheric H_2O concentration C^{H_2O}. In a plot, the two quantities are related by a straight line. The slope of this line depends on the details of the plant morphology. That is, at a given humidity, the studied species lose water at different rates.

The wind speed influences the results via the boundary layer thickness, which decreases with decreasing characteristic dimension (for a cylindrical structure its radius) and increasing wind speed. The boundary layer thickness governs the boundary layer conductance both for gaseous exchange and heat transfer (see review by Schuepp, 1993). The main resistance to gaseous exchange, however, is contributed not by the boundary layer, but by the low stomatal density of rhyniophytic plants, and variation of wind speed has thus a low or even no effect on the gas fluxes through the stomata (see Section 4.2). Convective heat transfer (heat is carried away by air movements), however, does not depend on stomatal conductance and is therefore strongly influenced by wind speed.

The process of heat transfer was not included in the present simulations. We assumed instead from the outset that the temperature of the axis is similar to air temperature. The justification for this assumption is as follows. Heat transfer via convection (sensible heat) and evaporative cooling due to transpiration (latent heat) represent important mechanisms for heat transfer in plants (see, for example, Gates, 1980; Monteith and Unsworth, 1990). Evaporative cooling is, however, of little importance for rhyniopyhtic plants due to the high stomatal resistance leading to low transpiration rates and it is therefore to be expected that convective cooling dominates heat transfer in rhyniophytic plants (Roth-Nebelsick, 2001). During low wind speed or calm air, the temperature of the plant axis, if exposed to direct sunlight, can reach values which are several degrees higher than air temperature (Roth-Nebelsick, 2001). Higher wind speeds ($u_{atm} \gtrapprox 0.5\ldots1$ m/s) lead to effective convective cooling of the cylindrical plant axis, because the intensity of this exchange process varies inversely to the boundary layer thickness, which is small for a body with a low characteristic dimension (Beerling et al., 2001; Roth-Nebelsick, 2001). Thus, under the conditions of the initial data set, the temperature of the rhyniophytic plant axis should approach the air temperature.

4.1.2. Biochemical parameters

All biochemical parameters have to be taken from extant plants. These parameters, together with the chloroplast surface factor (see Section 2.2 and Appendix), represent an outstanding factor of uncertainty. The extent of uncertainty to be faced depends on whether a parameter is 'critical', that is, whether small changes of the parameter have significant influence on the results or not. In the latter case, an accurate knowledge of the value of this parameter is less crucial. Such sensitivity analyses show that the chloroplast surface factor $\{a_{chl}/a_{as}\}$ as well as V_{max} and J_{max} represent critical parameters whereas the other parameters are far less crucial (see Sections 3.3.1, 3.3.4 and Fig. 8).

The values for V_{max} and J_{max} of the initial data set are chosen according to two criteria: they are typical for plants belonging to phylogenetic older groups, such as conifers or cycads. In order to narrow this range, we fine-tuned V_{max} and J_{max}

in such a way, that the ratio between the internal and the external CO_2 concentrations amounts to $C_i/C_a = 0.7$. How reliable this choice is, if applied to rhyniophytic plants, will be discussed in the following.

(1) It is generally assumed that rhyniophytic plants were C_3 plants (Raven, 1993). Furthermore, the properties of photosynthetic enzymes appear to be rather similar among extant plants (Badger and Andrews, 1987; Bowes, 1993). It is therefore to be expected that the kinetic properties of Rubisco in early land plants were similar to those being measured in extant C_3 plants. It appears thus justified to use values of the extant spectrum.

(2) The question arises which values of V_{max} and J_{max} of the extant spectrum should be used. Rhyniophytic plants evolved in an atmosphere with outstandingly higher atmospheric CO_2 concentrations compared to Recent conditions. Under extant atmospheric conditions, the Rubisco of those plants utilizing mechanisms which result in higher CO_2 concentrations at the carboxylation site (such as C_4 and CAM plants or aquatic plants with CO_2 concentrating mechanisms) shows a lower affinity to CO_2 than the Rubisco of C_3 plants with lower CO_2 concentrations at the carboxylation site. It is thus not to be expected that early land plants which evolved under high CO_2 showed assimilation parameters of high performance C_3 plants which evolved under much lower atmospheric CO_2 concentrations. Using values located at the lower range of the extant spectrum thus appears to be justified.

(3) $C_i/C_a = 0.7$ is generally considered as representing a common value among vascular plants (Robinson, 1994; Beerling and Woodward, 1997; Larcher, 1997). Numerous species do actually show this value during photosynthesis (von Caemmerer and Evans, 1991; Franks and Farquhar, 1999). It is, however, not strictly obeyed by plants and in many cases the C_i/C_a ratio can deviate significantly from 0.7 (Farquhar et al., 1989; Franks and Farquhar, 1999). It is not clear whether $C_i/C_a = 0.7$ was also obeyed by early land plants which evolved and existed under completely different external CO_2 concentrations if compared to Recent conditions. Robinson (1994) suggested that steeper gradients of CO_2 from the outside to the intercellular air spaces may have been maintained by plants living under higher atmospheric CO_2 concentrations than today. Nonetheless, applying the $C_i/C_a = 0.7$ criterion to early land plants results in reasonable assimilation rates (see Section 4.3). According to these considerations, we choose the values of V_{max} and J_{max} in the initial data set such that a ratio $C_i/C_a = 0.7$ is maintained. Substituting instead values from *Picea abies* for V_{max} and J_{max} leads in the case of *Rhynia* to a ratio which hardly deviates from $C_i/C_a = 0.7$. For *Aglaophyton* and *Nothia*, however, the *P. abies* values lead to steep CO_2 gradients: the ratios C_i/C_a amount to $C_i/C_a = 0.42$ (*Aglaophyton*) and $C_i/C_a = 0.35$ (*Nothia*), and the assimilation rates are twice as high as is the case for $C_i/C_a = 0.7$ (see Fig. 6). The rather constant values of $\delta^{13}C$ of terrestrial organic matter since the Devonian, however, indicate that the ratio of C_i/C_a was more or less constant through time (Edwards et al., 1998).

4.2. Transpiration of the rhyniophytic axes

Significant differences in transpiration rate exist between the considered taxa (Fig. 4). These differences are only due to anatomical and morphological properties. *Nothia* shows the highest water loss rate due to the high stomatal density and the lack of narrow hypodermal channel underneath the stomata. Relating transpiration rate to surface area, however, does not provide any information about the differences in the degree of water loss in cylindrical plant axes with different radii. With the same transpiration rate per surface area, the parenchyma of a thicker axis loses a smaller fraction of water than the parenchyma of a thinner axis. This is because the volume of a plant axis increases with the radius squared while the transpiring surface area increases proportional to the radius. If the transpiration rate is related to volume, then the transpiration rate of *Aglaophyton* is significantly lower than that for *Rhynia* and much lower than that for *Nothia*. *Aglaophyton* thus shows a significantly more strict water conservation strategy than *Rhynia* and *Nothia*.

The position of the stomata in *Nothia*, on the summits of the emergences, and the surface roughening due to these emergences were interpreted as increasing transpiration rate, because: (1) the exposed position of the stomata would cause the pore to be positioned outside the low velocity region of the boundary layer, and (2) a rough surface promotes a turbulent boundary layer (Kerp et al., 2001). The boundary layer does, however, not represent the main diffusive resistance for gaseous exchange. The following ratios of resistances res (inverse of conductance *S*) are valid for diffusion of both CO_2 and H_2O: (bl = boundary layer, st = stomatal layer, hy = hypodermal layer, if present, as = assimilation layer) $res_{bl}:res_{st}:res_{hy}:res_{as} = 1:5560:1037:7$ for *Aglaophyton*, 1:6166:1144:7 for *Rhynia* and $res_{bl}:res_{st}:res_{as} = 1:73\,682:5$ for *Nothia*. Reducing the boundary layer resistance (i.e. increasing the boundary layer conductance) thus does not influence gaseous exchange significantly, neither in *Aglaophyton* and *Rhynia* nor in *Nothia*. It is therefore improbable that the rough surface of *Nothia* increased gaseous exchange. An unequivocal interpretation of possible functional features of the emergences of *Nothia* is difficult at present. It could be speculated that these structures possibly played a role in heat transfer because heat transfer is (1) mainly independent of stomata and the gas fluxes through them, and (2) sensitive to boundary layer thickness and turbulence.

The strict water-conserving strategy of *Aglaophyton* and – to a lower extent – in *Rhynia* is in accordance with information available about the growth form of these plants. *Aglaophyton* and *Rhynia* do not show massive underground rhizom systems and the ability of *Aglaophyton* and *Rhynia* with respect to water absorption was probably severely restricted despite the fact that both taxa occurred in more humid habitats (there is, for example, evidence that *Aglaophyton* was able to survive flooding events, see Remy and Hass, 1996). Transpiration rate could additionally be decreased by stomatal closure during, for example, periods of high plant-to-air vapor pressure deficits, as shown in Fig. 10b.

The effects of mycorrhizal fungi which are present in many rhyniophytic taxa cannot yet be fully assessed. Mycorrhizal fungi are usually interpreted as improving the nutrient supply as is the case in extant mycorrhizas (Harley and Smith, 1983; Taylor et al., 1992; Taylor and Taylor, 1997). There is evidence that in some cases extant mycorrhizae may contribute also to the water supply of the host plant (Ruiz-Lozano and Azcon, 1995). It is, however, unclear whether this also occurred in rhyniophytic plants to a significant amount.

The role of mycorrhizae on gaseous exchange in rhyniophytic plants – except of decreasing the size of intercellular voids by settlement of fungal hyphae – is difficult to estimate until more studies are made. At any rate, water conservation was very probably of utmost importance for rhyniophytic plants (Edwards et al., 1998).

The higher transpiration rate of *Nothia* (which is still low compared to common transpiration rates of extant plants) is also supported by fossil data. *Nothia* showed an extensive underground rhizom system. This massive rhizomatous system of *Nothia* shows clusters of rhizoids being directly connected to the stele of the aerial axes (Kerp et al., 2001). This indicates that *Nothia* probably had a better water-absorbing capacity than *Aglaophyton* and *Rhynia* and could thus sustain the comparatively high transpiration rate of the aerial system. Additionally, the aboveground axes probably had a short life span and were shedded during unfavorable (dry?) periods whereas *Aglaophyton* and *Rhynia* possessed more long-living axes. This is indicated by the poorer preservation potential of the aerial axes of *Nothia* compared to *Aglaophyton* and *Rhynia*.

4.3. Assimilation of the rhyniophytic axes

With the initial data set, the assimilation rates of *Aglaophyton*, *Rhynia* and *Nothia* (related to projected surface area) are 14.4 μmol/m^2/s (*Aglaophyton*), 16.1 μmol/m^2/s (*Rhynia*) and 23.1 μmol/m^2/s (*Nothia*), respectively. That is, they lie in the lower to middle range of values of net photosynthesis usually found in extant plants (see, for example, Long et al., 1993; Larcher, 1997). Extant plants with very low assimilation rates, such as the ferns *Osmunda regalis* and *Pteridium aquili-*

num, show values in the range 10...12 μmol/m^2/s under optimal conditions (Franks and Farquhar, 1999). Typical values of conifers lie in the range of 6...10 μmol/m^2/s and the morphological and anatomically similar extant species *Psilotum nudum* shows characteristic assimilation rates of 2.5 μmol/m^2/s (Long et al., 1993; Larcher, 1997). The rhyniophytic values are caused by the high external CO_2 concentration leading to saturation of photosynthesis. Calculations carried out by Raven (1993) who also demonstrated that saturated photosynthesis occurred in rhyniophytic plants, arrived at even higher values of about 94 μmol/m^2/s and he described this value as representing a possible maximum. This value is based, however, on maximum photosynthesis rate per exposed internal cell area of extant leaves and is thus not fully comparable to the present approach. Beerling et al. (2001) presented values of about 10 μmol/m^2/s. It is, however, not clear whether these are expressed on a projected surface area basis. The high WUE values of the three taxa which are about 20 times higher than typical WUE values of extant mesophytic plants are due to the low transpiration rates.

More germane to rhyniophytic plants than assimilation per surface area, however, is the CO_2 influx per plant volume. The energetic demand of the plant is not proportional to its surface but to the amount of living tissue and thus to the volume of the plant. The assimilation process has to take place at the peripheral region of the cylinder, because light and gas cannot penetrate further than to a certain depth of the tissue (Niklas, 1997). For the cylindric shape, the volume (proportional to the amount of energy consuming tissue) increases with the radius squared while the surface (proportional to the amount of energy producing assimilation tissue) increases proportional to the radius (see also Section 4.2). The energy-consuming volume thus increases stronger with radius than the energy producing surface. If assimilation rates obtained with the initial data set are represented as rates per volume then *Aglaophyton* shows the lowest and *Nothia* the highest value (see Fig. 5).

In the case of *Aglaophyton* and *Rhynia*, the assimilation rates obtained during the calculations appear to be more than sufficient for maintaining the plants since both taxa show neither an extensive rhizome system which has to be supported by the aerial axes nor costly support tissues, because rhyniophytic plants were turgor-stabilized (Speck and Vogellehner, 1988). In perennial plants, half of the carbohydrate products are consumed by the root system and by building tissues for structural support (Givnish, 1979; Raich and Nadelhoffer, 1989). *Nothia* shows a massive rhizom system representing a carbohydrate sink which indicates a demand for higher assimilation rate in *Nothia*. Moreover, the apparently seasonal occurrence of the aerial axes of *Nothia* can be interpreted as intensifying a demand for their high productivity. That *Nothia* exhibits in all cases the highest assimilation rate is therefore corroborated by information provided by the fossil record.

For all three taxa, saturation of photosynthesis was probably important in order to obtain sufficient carbohydrate gain. Saturation of photosynthesis is dependent on: (1) the external CO_2 concentration, and (2) anatomical parameters, mainly stomatal density ν_{st}. It is obvious from Fig. 9a (assimilation rate per volume plotted against d_{hc} and ν_{st}) that with the initial data set (and also with the *Picea abies* set of J_{max} and V_{max}) the (calculated) threshold values of ν_{st} leading to saturated photosynthesis in *Aglaophyton* are close to their actual stomatal densities which are obtained from fossilized specimen. Decreasing ν_{st} significantly would strongly decrease the assimilation rate, because photosynthesis would no longer be saturated. Fig. 11 shows that the WUE value of the initial data set is seated at the beginning of the steep flank leading to maximum WUE. In the light of Fig. 10a (showing transpiration rate plotted against d_{hc} and ν_{st}), the 'actual' stomatal density of *Aglaophyton* appears to represent a compromise between transpiration and assimilation, leading to an optimized gaseous exchange. Simulation of stomatal closure for *Aglaophyton* demonstrated that – with the initial data set – transpiration can be strongly reduced by closing the stomatal pore while assimilation remains largely unaffected (Figs. 9b and 10b). Actual WUE values could thus be even larger in rhyniophytic plants, with photosynthesis being saturated.

Fig. 13a,b shows that saturation can be achieved over a wide range of combinations of C_a and v_{st} values. Higher C_a values than in the initial data set allow lower values of v_{st} while assimilation stays saturated. It is usually difficult to detect stomata on fossilized axes of early land plants dating further back than to the Lower Devonian (Edwards, 1998). Since the atmospheric CO_2 content during the Silurian was even higher than during the Lower Devonian (Berner and Kothvala, 2001), the results summarized in Fig. 13a,b suggest that plant axes of this ancient age could survive with a very low stomatal density, drastically reducing the probability of their detection. Fig. 13a,b also shows that decreasing C_a leads eventually to a regime in which a strong increase in v_{st} is necessary in order to allow for saturated photosynthesis. The strong decrease of atmospheric CO_2 content during the Middle Devonian may thus be involved in the disappearance of rhyniophytic plants during this time period, because they were probably not able to adapt their stomatal densities to these new conditions.

The results summarized so far indicate that the actual values of stomatal density (together with the depth of the hypodermal channels, if present) represent a fine-tuning of gaseous exchange which integrates maximum carbon gain and minimum transpiration rate to a compromise solution of optimized gas fluxes. This optimum also reflects the limited capacity of water absorption in rhyniophytic plants. Rhyniophytic plants represent an ancient construction originating in the colonization process of terrestrial environments by green plants (Edwards, 1998). The low and optimized values of gaseous exchange are very probably a consequence of the restricted water-absorbing capacity, and it is therefore possible that the high atmospheric CO_2 concentrations were required in order to 'permit' the evolution of upright terrestrial plants (Edwards et al., 1998). On the one hand, rhyniophytic plants were, as indicated by the results, excellently adapted to early Paleozoic conditions. On the other hand, the high atmospheric CO_2 conditions were probably the fundamental precondition for the evolution of the rhyniophytic habit.

4.4. Implications of the results for atmospheric CO_2 concentration of the Lower Devonian

The structure of Fig. 13a – an extended plain lowland representing saturated photosynthesis framed on two sides by the continuously ascending slopes of undersaturated photosynthesis – contributes additional information for determining the CO_2 concentration of the Lower Devonian atmosphere.

Consider a hypothetical plant X with stomatal density v_X living in an atmosphere with CO_2 concentration C_X. If the values of v_X and C_X give X a position somewhere within the 'lowland of saturation', X has reached its optimum conditions with respect to assimilation. Its performance with respect to transpiration, however, would obviously be better at smaller values of v_X, as can be seen from Fig. 11. Therefore, we may expect that X exhibits a tendency to occupy a position with as low v_X values as possible without impairing photosynthesis saturation. This evolutionary optimum is obviously realized by a v_X value on the borderline between the 'lowland of saturation' and the 'slopes of undersaturated photosynthesis'.

In order to determine the CO_2 concentration of the Lower Devonian atmosphere from the known stomatal density $v_{rhyniophyte}$ of the rhyniophytes, we can turn this argument around (see Fig. 13b): on the premises that the rhyniophytes were well adapted to their environment the Lower Devonian CO_2 concentration can be found from the position where a straight line at $v_{st} = v_{rhyniophyte}$ parallel to the abscissa intersects the borderline separating saturated and undersaturated photosynthesis. This 'cut' through Fig. 13b is represented by Fig. 12a. The shape and extent of the area of saturated photosynthesis in Fig. 13a,b depend, however, on the choice of the assimilation parameters, especially of J_{max} and V_{max}. The sensitivity analysis described in Section 3.3.1 demonstrates the effects of changing J_{max} and V_{max}. In this sensitivity study, values of J_{max} and V_{max} of an extant plant (*Picea abies*) were inserted (effect on assimilation shown by Figs. 6 and 12b); then the construction just given leads to three different optimum values for the atmospheric CO_2 concentration: $C_a \approx 166$ mmol/

m^3 (*Aglaophyton*), $C_a \approx 193$ mmol/m^3 (*Nothia*) and $C_a \approx 106$ mmol/m^3 (*Rhynia*, see Fig. 12b). In this case, the range of plausible atmospheric CO_2 concentrations is thus $C_a \approx 106...193$ mmol/m^3. The assimilation parameters of *Picea* result, however, in extremely low values of C_i/C_a: 0.42 for *Aglaophyton* and 0.35 for *Nothia*. It is therefore reasonable to assume that the values of the initial data set which result in $C_i/C_a = 0.7$ represent a good approximation. If we thus impose – in view of the discussion in Section 4.1.2 – the initial data set in order to fine tune the values of J_{max} and V_{max}, then we obtain $C_a \approx 120$ mmol/m^3 which is about 8.5 times the Recent value. It is lower than the value provided by the standard curve of R_{CO_2} returned by GEOCARBIII, which is about 12 times the Recent value (Berner and Kothvala, 2001). McElwain (1998) provided two estimations of atmospheric CO_2 of the Lower Devonian based on stomatal densities of the Lower Devonian plants *Sawdonia ornata* and *Aglaophyton major*: the first one amounts to a range $R_{CO_2} = 7...10$ (by using a 'Recent standard') and the second one gives a range $R_{CO_2} = 9.5...12.5$ (by using a 'Carboniferous standard'). The estimation obtained by the present contribution is thus seated within the first range. It should, however, be noted that the method applied by McElwain (1998) is based on producing ratios between the stomatal densities of the fossil taxon and an extant plant species termed 'NLE' (nearest living equivalent) whose ecological and structural properties are claimed to be similar to those of the fossil taxon. Additionally, the value of stomatal density of *Aglaophyton* which were used by McElwain (1998) ($v_{st} = 4.5/mm^2$) is much higher than the stomatal density which was applied in this contribution (McElwain and Chaloner, 1995; McElwain, 1998, see also Edwards et al., 1998). The data of stomatal density available so far show some variation. As indicated in Table 2, the anatomical parameters provided by Edwards et al. (1998) and Kerp et al. (2001) as well as their data on stomatal density were used in order to create a consistent data set. A direct comparison of the present results and the results of McElwain (1998) thus appears to be problematic.

5. Conclusions

(1) The three considered taxa differ in transpiration and assimilation rate and show the following order of increasing gaseous exchange provided the condition $C_i/C_a = 0.7$ is applied: *Aglaophyton major* < *Rhynia gwynne-vaughanii* < *Nothia aphylla*. The transpiration rates of all three taxa are markedly lower than the rates which are usually attained by extant plants. The assimilation rates are seated at the lower to middle range of the extant spectrum due to photosynthesis saturation under Lower Devonian CO_2 concentrations.

(2) The fact that *Nothia aphylla* shows the highest rates of gaseous exchange is consistent with the fact that this species developed a massive rhizom system which represented very probably a carbon sink on one hand while providing a much better source of water supply than was present in *Aglaophyton major* and *Rhynia gwynne-vaughanii* on the other hand. The fossil evidence of seasonally shedding of the aerial axes of *N. aphylla* additionally indicates a demand for higher productivity of these axes during their lifetime.

(3) The protuberances at the axis surface of *Nothia aphylla* did not increase gaseous exchange.

(4) The differences in gaseous exchange of the three taxa thus probably reflect differences in their lifestyles and ecophysiological properties.

(5) The results indicate on one hand that the construction of rhyniophytic plants is strongly adapted to a high atmospheric CO_2 concentration by producing optimized gaseous exchange. This means, however, on the other hand that the evolution and existence of rhyniophytic plants – and therefore the prototype of land plants with an upright posture – was dependent on such high CO_2 concentrations.

(6) The results concerning interrelationship between fine-tuning of gaseous exchange, assimilation rate, anatomical properties and external CO_2 concentration suggest that the Lower Devonian CO_2 concentration amounted roughly to about $C_a \approx 120$ mmol/m^3.

6. Glossary

see also Tables 1–3.

Environmental and physical parameters and constants

A	assimilation rate per volume
C	gas concentration
C_i	intercellular CO_2 concentration
C_a	atmospheric CO_2 concentration
C^{CO_2}	atmospheric CO_2 concentration
C^{H_2O}	atmospheric H_2O concentration, humidity
D	free air diffusional constant
D^{CO_2}	free air diffusional constant for CO_2
D^{H_2O}	free air diffusional constant for H_2O
d_{bl}	thickness of boundary layer
grad	gradient operator
$\vec{j}$	diffusional gas flux
f^{CO_2}	assimilation rate per area
f^{H_2O}	transpiration rate per area
I	irradiance
l	path length
l_e	path length around hindrance
n	porosity
Q	gas sink
r	radial coordinate
R_{CO_2}	fossil CO_2 concentration/Recent CO_2 concentration
R_{gas}	universal gas constant
S	effective conductance
$S_\odot$	solar constant
τ	tortuosity
T	absolute temperature
$\mathcal{T}$	transpiration rate per volume
u_{atm}	wind velocity

Anatomical and morphological parameters

A	total leaf surface
A^{chl}	total area of all chloroplasts
A^{mes}	total area of all mesophyll cells
a_{as}	surface of cortex cell
a_{chl}	surface of all chloroplasts in a cell
A_η	surface of a chloroplast
a_{st}	area of stomatal pore
d_{st}	depth of stomatal pore
d_{hc}	length of hypodermal channel
h_{hc}	long axis of hypodermal channel
L	axis length
n_{as}	porosity of assimilation layer
n_{st}	porosity of stomatal layer
R	radius of plant axis
R_c	length of longer axis of chloroplast
V	tissue volume
V_p	tissue pore volume
η	ratio of chloroplast thickness and chloroplast length
v_{as}	volume of cortex cell
w_{hc}	short axis of hypodermal channel
v_{st}	stomatal density
ρ	effective pore radius
σ	radius of cortex cell
τ_{st}	tortuosity of stomatal layer

Photosynthesis parameters

g_{liq}	effective conductance through a cortex cell
J	current of molecules
j	flux into plant surface
j_{as}	flux into assimilating tissue
j_{chl}	flux into chloroplast
$J(I)$	potential rate of electron transport
J_{max}	light-saturated rate of electron transport
K_c	Michaelis–Menten constant of carboxylation
K_o	Michaelis–Menten constant of oxygenation
p_o	Partial pressure of oxygen at assimilating site
q	partial pressure of CO_2 at assimilating site
V_{max}	local maximum carboxylation rate
W_c	carboxylation rate limited by Rubisco activity
W_j	carboxylation rate limited by Rubisco regeneration
α	efficiency of light conversion
θ	specificity factor of Rubisco

Acknowledgements

This work was supported by the German Science Foundation (DFG: Mo 412/13;c-1). We want to thank H. Kerp and H. Hass for many helpful discussions and J.H. Nebelsick for critically reading the English manuscript.

Appendix A

A.1. Photosynthesis model

The CO_2 flux into chloroplasts, j_{chl}, is given by

$$j_{chl}(q,I) = \left(1-\frac{p_o}{2\theta q}\right)\min\{W_c(q), W_j(q,I)\} \quad (5)$$

with

$$W_c(q) := V_{max}\frac{q}{q + K_c\left(1+\frac{p_o}{K_o}\right)}$$

$$W_j(q,I) := J(I)\frac{q}{4\left(q+\frac{p_o}{\theta}\right)} \quad (6)$$

and

$$J(I) := = \frac{\alpha I}{\sqrt{1+\left(\frac{\alpha I}{J_{\max}}\right)^2}} \quad (7)$$

where q stands for the partial pressure of CO_2 and p_o for the local O_2 concentration (the various other parameters are listed in Table 3 and in the glossary).

The expression $\min\{W_c(q), W_j(q,I)\}$ denotes the smaller of $W_c(q)$ (carboxylation rate limited by the activity of Rubisco) and $W_j(q,I)$ (carboxylation rate limited by regeneration of Rubisco via electron transport).

j_{chl} is connected to Q by the following equation:

$$Q = -\left(\frac{a_{chl}}{a_{as}}\right)\left(\frac{a_{as}}{v_{as}}\right)(1-n_{as})j_{chl}(q,I) \quad (8)$$

with the ratio a_{chl}/a_{as} between the sum of the surfaces of all chloroplasts within one cortex cell to the surface a_{as} of this cell (termed 'chloroplast surface factor' throughout the text), the porosity n_{as} of the assimilation layer and a_{as}/v_{as} as the surface-to-volume ratio of a typical cortex cell. Eq. 8 thus states that the sink is produced by the chloroplast layer located at the periphery of a cortex cell. A final step is required which converts the partial pressure q of CO_2 inside the chloroplasts in Eq. 7 into the CO_2 concentration $C(r)$ in the intercellular air spaces (Parkhurst and Mott, 1990):

$$j_{chl} = g_{liq}(C(r)R_{gas}T - q) \quad (9)$$

where R_{gas} represents the universal gas constant, T the absolute temperature and g_{liq} the effective conductance through the interior structures of the cortex cells (see Fig. 14 for a schematic overview of the model).

A.2. Boundary layer

The thickness of the boundary layer (air layer with reduced wind velocity) adjacent to the axis surface is determined according to an approximation provided by Nobel, 1999:

$$d_{bl} = 5.8\ mm\sqrt{\frac{2R}{u_{atm}}\frac{1}{s}} \quad (10)$$

with d_{bl} the thickness of boundary layer, R the radius of the plant axis, and u_{atm} the wind velocity.

A.3. Stomatal layer

Permineralized specimen of *Aglaophyton*, *Nothia* and *Rhynia* provide the necessary anatomical data: average area of stomatal pore a_{st}, depth of stomatal pore d_{st} and number of stomata per unit surface v_{st}. These parameters are used in order to calculate porosity n_{st} and tortuosity τ_{st} of the stomatal layer:

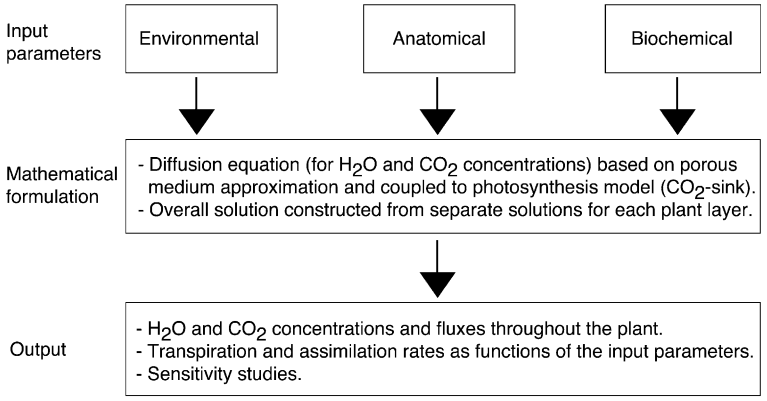

Fig. 14. Schematic overview of the model.

$$n_{st} = a_{st} v_{st} \tag{11}$$

$$\tau_{st} = 1 + \frac{\rho_{st}}{d_{st}} \tag{12}$$

with ρ_{st} the effective pore radius (see Nobel, 1999). The tortuosity stems from the fact that lines of equal concentration within the boundary layer bulge out over the stomata so that molecules diffusing out of the stomata still experience stomatal conditions although they have already left the stomatal layer (Nobel, 1999).

A.4. Hypodermal layer

A hypodermal layer is included in the system, if hypodermal channels are present. These structures are narrow channels beneath the stomata and can be found in *Aglaophyton* and *Rhynia*. *Nothia* has substomatal chambers. Hypodermal channels are elliptical in cross-section with a longer axis h_{hc} and a shorter axis w_{hc}. Their number equals the number of stomata. The porosity of the hypodermal layer reads as:

$$n_{hy} = \frac{\pi}{4} h_{hc} w_{hc} v_{st} \frac{2R - d_{st}}{2R - (2d_{st} + d_{hy})} \tag{13}$$

A.5. Assimilation layer

It is generally assumed that assimilation took place mainly in the outer cortex (see, for example, Edwards et al., 1998). The assimilation layer is therefore represented by the outer cortex layer. Measurements carried out by using methods of image processing on thin slices of fossil material yield an average value for porosity of $n_{as} = 0.35$ for all three taxa. For measured thickness values of the outer cortex layer of the three taxa see Table 2. In order to calculate the tortuosity τ_{as}, a rough approximation is applied: a molecule diffusing around a cell has to move along a half circular path with a distance r to the cell center. The pathlength l_e amounts to $l_e = r$ and the direct travel distance is $l = 2r$. The tortuosity is therefore given by:

$$\tau_{as} = \frac{l_e}{l} = \frac{\pi}{2} \approx 1.57 \tag{14}$$

The specific surface (a_{as}/v_{as}) of a long cylindrical cortex cell with radius σ reads as:

$$\left(\frac{a_{as}}{v_{as}}\right) = \frac{2}{\sigma} \tag{15}$$

The ratio (a_{chl}/a_{as}) represents the sum of the surfaces of all chloroplasts a_{chl} within one cortex cell to the surface a_{as} of this cell. In a sense this value thus describes how much space of a cell is occupied by chloroplasts. The value is determined by two factors: (1) the orientation of the chloroplasts in the cell, and (2) the degree of (inner) surface occupation of the cell by chloroplasts. Typical chloroplasts of land plants are similar to oblate spheroids. The surface of a chloroplast is then provided by

$$A_\eta = 2\pi R_c^2 + \pi R_c^2 \frac{\eta^2}{\sqrt{1-\eta^2}} \ln\left(\frac{1+\sqrt{1-\eta^2}}{1-\sqrt{1-\eta^2}}\right) \quad (0 \le \eta \le 1) \tag{16}$$

with R_c the length of the spheroid's longer axis and η the ratio of chloroplast thickness to chloroplast length. The shorter axes of typical chloroplasts of land plants are about half as long as their two longer axes. If the inner surface of a cortex cell would be completely occupied by these chloroplasts, CO_2 diffusing into one chloroplast would have to diffuse through a cortex cell area of πR_c^2. The ratio (a_{chl}/a_{as}) would then be given by (a_{chl}/a_{as}) = 2.760. Chloroplasts in land plants differ in size. Typical values are, according to Moore et al., 1998, 4...8 μm for the chloroplast diameter and 2...3 μm for the chloroplast thickness (see also Raven, 1993). We adopt the mean values of these two intervals and arrive at (a_{chl}/a_{as}) = 2.606 for $\eta = 0.429$. The inner cell surfaces of cells containing chloroplasts are, however, not completely occupied by these cell organelles. According to Parkhurst and Mott, 1990, a value of 90% which is typical for mesophyll cells of extant leaves is adopted. A value of

$$(a_{chl}/a_{as}) = 2.3454 \tag{17}$$

thus results which was used in the calculations.

A.6. V_{max} and J_{max}

Values of V_{max} and J_{max} provided in the literature cannot be applied directly, because the fluxes usually given are related to a fictitious external leaf area far away from the chloroplasts. In order to be used within the framework of our calculations, values from the literature have to be corrected for the actual A^{mes}/A values of the rhyniophytic plant. V_{max} and J_{max} are thus redefined according to the following considerations. Consider a current of molecules J diffusing into or out of the chloroplasts under stationary conditions. A^{chl}, A^{mes} and A represent the total areas of chloroplasts, of all mesophyll cells and of the total leaf surface. If the corresponding fluxes – the symbol j stands for either V_{max} or J_{max} – are defined by

$$j_{chl} := \frac{J}{A^{chl}} \quad j_{mes} := \frac{J}{A^{mes}} \quad j := \frac{J}{A} \tag{18}$$

then elimination of J results in

$$j_{chl} A^{chl} = j_{mes} A^{mes} = jA \tag{19}$$

and thus

$$j_{chl} = j\left(\frac{A}{A^{chl}}\right) = j\left(\frac{A}{A^{mes}}\right)\left(\frac{A^{mes}}{A^{chl}}\right) \tag{20}$$

Since $(A^{chl}/A^{mes}) = (a_{chl}/a_{as})$, we conclude

$$j_{chl} = j\left(\frac{A}{A^{mes}}\right)\left(\frac{a_{as}}{a_{chl}}\right) \tag{21}$$

Own measurements of (A^{mes}/A) provided a value of $(A^{mes}/A) = 10$ and $(a_{chl}/a_{as}) = 2.3454$ has been calculated above. The local values of V_{max} and J_{max} can now be obtained by substituting the appropriate literature data of V_{max} or J_{max} for j on the right hand side of Eq. 21.

A.7. Irradiance

The value of the Recent solar constant $S_{\odot}$ amounts to $S_{\odot} = 1360$ W/m^2 (see, for example, Nobel, 1999). About 45% of this amount is absorbed in the upper atmospheric layers or reflected back into space. On a global average, 55% thus reaches the earth's surface. About 45% of this amount of radiation is within the range of photosynthetically valuable wavelengths.

If the sun is elevated above the horizon by an angle Θ, the projective absorption area of an upright plant axis with a radius of R and a height of L is given by $2RL \cos \Theta$. On distributing the impinging light evenly onto the telome surface $2\pi RL$, the factors R and L drop out and the number I_{Θ} of photons reaching the axis per unit time and unit axis area is given by:

$$I_{\Theta} = \cos \Theta \times 877 \frac{\mu mol}{m^2\ s} \tag{22}$$

Assuming $\Theta = 45°$ and taking into account differences in the inner structures of *Aglaophyton*, *Rhynia* and *Nothia*, we arrive at an expression between I_{Θ} and the number I of photons at the assimilating sites per unit time and unit area, which is similar to the one obtained above for the relation between j and j_{chl}:

$$I = I_{\Theta}\left(\frac{A}{A^{mes}}\right)\left(\frac{a_{as}}{a_{chl}}\right) \tag{23}$$

References

Aphalo, P.J., Jarvis, P.G., 1993. An analysis of Ball's empirical model of stomatal conductance. Ann. Bot. 72, 321–327.

Badger, M.R., Andrews, T.J., 1987. Co-evolution of Rubisco and CO_2 concentrating mechanisms. In: Biggins, J. (Ed.), Progress in Photosynthesis Research. Martinus Nijhoff, Dordrecht, pp. 501–609.

Ball, J.T., Woodrow, I.E., Berry, J.A., 1987. A model predicting stomatal conductance and its contribution to the control of photosynthesis under different environmental conditions. Biggins, J. (Ed.), Progress in Photosynthesis Research. Martinus Nijhoff, Dordrecht, pp. 221–224.

Bateman, R.M., Crane, P.R., DiMichele, W.A., Kenrick, P., Rowe, N.P., Speck, T., Stein, W., 1998. Early evolution of land plants: phylogeny, physiology, and ecology of the primary terrestrial radiation. Annu. Rev. Ecol. Syst. 29, 263–292.

Becker, M., Kerstiens, G., Schönherr, J., 1986. Water permeability of plant cuticles: permeance, diffusion and partition coefficients. Trends Ecol. Evol. 1, 54–60.

Beerling, D.J., Woodward, F.I., 1995. Leaf stable carbon isotope composition records increased water-use efficiency of C_3 plants in response to atmospheric enrichment. Funct. Ecol. 9, 394–401.

Beerling, D.J., Woodward, F.I., 1997. Changes in land plant function over the Phanerozoic: reconstructions based on the fossil record. Bot. J. Linn. Soc. 124, 137–153.

Beerling, D.J., Osborne, C.P., Chaloner, W.G., 2001. Evolution of leaf from in land plants linked to atmospheric CO_2 decline in the late Palaeozoic era. Nature 419, 352–354.

Berner, R.A., Kothvala, Z., 2001. GEOCARBIII: A revised model of atmospheric CO_2 over Phanerozoic time. Am. J. Sci. 301, 182–204.

Bowes, G., 1993. Facing the inevitable: Plants and increasing atmospheric CO_2. Annu. Rev. Plant Physiol. Plant Mol. Biol. 44, 309–332.

Cowan, I.R., Farquhar, G.D., 1977. Stomatal function in relation to leaf metabolism and environment. Symp. Soc. Exp. Biol. 31, 471–505.

Edwards, D., 1993. Tansley Review No. 53. Cells and tissues in the vegetative sporophytes of early land plants. New Phytol. 125, 225–247.

Edwards, D., 1998. Climate signals in Palaeozoic land plants. Philos. Trans. R. Soc. London Ser. B 353, 141–157.

Edwards, D., Abbott, G.D., Raven, J.A., 1996. Cuticles of early land plants: a palaeoecophysiological evaluation. In: Kerstiens, G. (Ed.), Plant Cuticles, an Integrated Functional Approach. ios Scientific Publishers, Oxford, pp. 1–31.

Edwards, D., Kerp, H., Hass, H., 1998. Stomata in early land plants: an anatomical and ecophysiological approach. J. Exp. Bot. 49, 255–278.

Edwards, D., Morel, E., Poiré, D.G., Cingolani, C.A., 2001. Land plants in the Devonian Villaricencio Formation, Mendoza Province, Argentina. Rev. Palaeobot. Palynol. 116, 1–18.

Farquhar, G.D., von Caemmerer, S., Berry, J.A., 1980. A biochemical model of photosynthetic CO_2 assimilation in leaves of C_3 species. Planta 149, 78–90.

Farquhar, G.D., Ehleringer, J.R., Hubick, K.T., 1989. Carbon isotope discrimination and photosynthesis. Annu. Rev. Plant Physiol. Plant Mol. Biol. 40, 503–537.

Franks, P.J., Farquhar, G.D., 1999. A relationship between humidity response, growth form and photosynthetic operating point in C_3 plants. Plant Cell Environ. 22, 1337–1349.

Gates, D.M., 1980. Biophysical Ecology. Springer Verlag, New York.

Gerrienne, P., Bergamaschi, S., Pereira, E., Rodrigues, M.-A.C., Steemans, P., 2001. An Early Devonian flora, including *Cooksonia*, from the Parana' Basin (Brazil). Rev. Palaeobot. Palynol. 116, 19–38.

Givnish, T.J., 1979. On the adaptive significance of leaf form. In: Solbrig, O.T., Jain, S., Johnson, G.B., Raven, P.H. (Eds.), Topics in Plant Population Biology. Columbia University Press, New York, pp. 375–473.

Harley, P.C., Sharkey, T.D., 1991. An improved model of C_3 photosynthesis at high CO_2: Reversed O_2 sensitivity explained the lack of glycerate re-entry into the chloroplast. Photosynth. Res. 27, 169–178.

Harley, J.L., Smith, S.S., 1983. Mycorrhizal Symbiosis. Academic Press, New York.

Harley, P.C., Thomas, R.B., Reynolds, J.F., Strain, B.R., 1992. Modelling the photosynthesis of cotton grown in elevated CO_2. Plant Cell Environ. 15, 271–282.

Jones, H.G., 1992. Plants and Microclimate. Cambridge University Press, Cambridge.

Kenrick, P., Crane, P.R., 1997. The origin and early diversification of land plants: a cladistic study. Smithsonian Series in Comparative Evolutionary Biology. Smithsonian Institution Press, Washington, DC.

Kerp, H., Hass, H., Mosbrugger, V., 2001. New data on Nothia aphylla Lyon, 1964 ex El Saadawy et Lacey, 1979: a poorly known plant from the Lower Devonian Rhynie Chert. In: Gensel, P.G., Edwards, D. (Eds.), Plants Invade the Land: Evolutionary and Environmental Perspectives. Columbia University Press, Columbia, pp. 52–82.

Kerstiens, G., 1996. Cuticular water permeability and its physiological significance. J. Exp. Bot. 47, 1813–1832.

Kirschbaum, M.U.F., Farquhar, G.D., 1984. Temperature dependence of whole leaf photosynthesis in *Eucalyptus pauciflora* Sieb. ex Spreng. Aust. J. Plant Physiol. 11, 519–538.

Konrad, W., Roth-Nebelsick, A., Kerp, H., Hass, H., 2000. Transpiration and assimilation of Early Devonian land plants with axially symmetric telomes – simulations on the tissue level. J. Theor. Biol. 206, 91–107.

Kramer, P.J., 1983. Water Relations of Plants. Academic Press, New York.

Kürschner, W.M., 1996. Leaf stomata as biosensors of palaeoatmospheric CO_2 levels. Ph.D. thesis, Utrecht.

Larcher, W., 1997. Physiological Plant Ecology, 3rd edn. Springer Verlag, New York.

Long, S.P., Postl, W.F., Bolhár-Nordenkampf, H.R., 1993. Quantum yields for uptake of carbon dioxide in C_3 vascular plants of contrasting habitats and taxonomic groups. Planta 189, 226–234.

McElwain, J.C., 1998. Do fossil plants signal palaeoatmospheric CO_2 concentration in the geological past? Philos. Trans. R. Soc. London Ser. B 353, 83–96.

McElwain, J.C., Chaloner, W.G., 1995. Stomatal density and index of fossil plants track atmospheric carbon dioxide in the Palaeozoic. Ann. Bot. 76, 389–395.

Monteith, J.L., Unsworth, M.H., 1990. Principles of Environmental Physics. Edward Arnold, London.

Moore, R., Clark, W.D., Vodopich, D.S., 1998. Botany. McGraw-Hill, Boston.

Niklas, K.J., 1997. The Evolutionary Biology of Plants. University of Chicago Press, Chicago, IL.

Niklas, K.J., Kerchner, V., 1984. Mechanical and photosynthetical constraints on the evolution of plant shape. Paleobiology 10, 79–101.

Nobel, P.S., 1999. Physicochemical and Environmental Plant Physiology, 2nd edn. Academic Press, New York.

Parkhurst, D.F., 1994. Tansley Review No. 65. Diffusion of CO_2 and other gases inside leaves. New Phytol. 126, 449–479.

Parkhurst, D.F., Mott, K.A., 1990. Intercellular diffusion limits to CO_2 uptake in leaves. Plant Physiol. 94, 1024–1032.

Raich, J.W., Nadelhoffer, K.J., 1989. Belowground carbon allocation in forest ecosystems: Global trends. Ecology 70, 1254–1346.

Raven, J.A., 1984. Physiological correlates of the morphology of early vascular plants. Bot. J. Linn. Soc. 88, 105–126.

Raven, J.A., 1993. The evolution of vascular plants in relation to quantitative functioning of dead water-conducting cells and stomata. Biol. Rev. 68, 337–363.

Remy, W., Hass, H., 1996. New information on gametophytes and sporophytes of Aglaophyton major and inferences about possible environmental adaptations. Rev. Palaeobot. Palynol. 90, 175–193.

Robinson, J.M., 1994. Speculations on carbon dioxide starvation, Late Tertiary evolution of stomatal regulation and floristic modernization. Plant Cell Environ. 17, 345–354.

Roth-Nebelsick, A., 2001. Heat transfer of rhyniophytic plant axes. Rev. Palaeobot. Palynol. 116, 109–122.

Ruiz-Lozano, J.M., Azcon, R., 1995. Hyphal contribution to water uptake in mycorrhizal plants as affected by the fungal species and water status. Physiol. Plant. 95, 472–478.

Schuepp, P.H., 1993. Tansley Review No. 59. Leaf boundary layers. New Phytol. 125, 477–507.

Speck, T., Vogellehner, D., 1988. Biophysical examinations of the bending stability of various stele types and the upright axes of early 'vascular' plants. Bot. Acta 101, 262–268.

Stewart, W.N., Rothwell, G.W., 1993. Palaeobotany and the Evolution of Plants, 2nd edn. Cambridge University Press, Cambridge.

Taylor, T.N., Remy, W., Hass, H., 1992. Fungi from the Lower Devonian Rhynie Chert: Chytridiomycetes. Am. J. Bot. 79, 1233–1241.

Taylor, T.N., Taylor, E.L., 1997. The distribution and interactions of some Paleozoic fungi. Rev. Palaeobot. Palynol. 95, 83–94.

von Caemmerer, S., Evans, J.R., 1991. Determination of the average partial pressure of CO_2 in chloroplasts from leaves of several C_3 plants. Aust. J. Plant Physiol. 18, 287–306.

Wullschleger, S.D., 1993. Biochemical limitations to carbon assimilation in C_3 plants – a retrospective analysis of the A/C_i curves from 109 species. J. Exp. Bot. 44, 907–920.

Zimmermann, W., 1959. Die Phylogenie der Pflanzen. Fischer, Stuttgart.